

ON FUTURE CHANGES IN STRATOSPHERIC SUDDEN WARMINGS

by

Ryan P. Oates

A thesis submitted to the faculty of
The University of Utah
in partial fulfillment of the requirements for the degree of

Master of Science

Department of Atmospheric Sciences

The University of Utah

May 2013

Copyright © Ryan P. Oates 2013

All Rights Reserved

ABSTRACT

Traditionally, stratospheric sudden warming events (SSWs) are defined using a fixed threshold criterion. This criterion, however, may lead to spurious results if the climate of the underlying dataset is changing. In an attempt to overcome this potential shortcoming we develop alternative criteria to define such events and test these criteria using reanalysis and climate model data. Results show that under different future climate forcing scenarios the annual and monthly mean SSW frequency increase. This increase is most robust in early to mid-winter. We therefore conclude that under a changing climate there is a higher potential for winter cold air outbreaks for regions such as North America, Europe, and northern Asia.

TABLE OF CONTENTS

| | |
|---|-----|
| ABSTRACT | iv |
| ACKNOWLEDGMENTS | vii |
| 1. INTRODUCTION | 1 |
| 1.1 The Stratospheric Polar Vortex | 1 |
| 1.2 Literature Review and Objectives | 7 |
| 2. DATA AND METHODS | 15 |
| 2.1 Data | 15 |
| 2.1.1 Observationally-Based Data | 15 |
| 2.1.2 Model Data | 15 |
| 2.2 Methods | 18 |
| 2.2.1 NAM Index | 18 |
| 2.2.2 Eliassen-Palm Flux | 19 |
| 2.3 Approaches Used To Define SSWs | 20 |
| 2.4 March SSW criterion | 27 |
| 2.5 Testing For Statistical Significance | 27 |
| 3. ANALYSIS | 29 |
| 3.1 Reanalysis and Model Control Runs | 29 |
| 3.1.1 Zonal-Mean Zonal Wind Comparison | 29 |
| 3.1.2 Zonal-Mean Zonal Wind Climatology | 29 |
| 3.1.3 Mean Seasonal Variability | 32 |
| 3.2 SSW Annual Frequency Summaries | 33 |
| 3.3 Monthly SSW Frequency Response | 36 |
| 3.4. Model Forcing Scenarios | 42 |
| 3.4.1 Zonal-Mean Zonal Wind Climatology | 43 |
| 3.4.2 Mean Seasonal Variability | 45 |
| 3.5 Annual SSW Frequency Comparison | 47 |
| 3.5.1 SSW Annual Frequency Summaries | 47 |
| 3.5.2 Monthly SSW Frequency Response | 49 |
| 3.6 SSW Dynamical Response to Forcing Scenarios | 57 |
| 3.7 Analysis and Comparison of C20R and NCEP-NCAR Reanalysis Data | 63 |

| | |
|--------------------------------|----|
| 4. SUMMARY AND DISCUSSION..... | 66 |
| REFERENCES | 71 |

ACKNOWLEDGMENTS

I would like to thank my advisor, Thomas Reichler, for his advice and guidance. I would also like to thank Paul Staten and Junsu Kim for their willingness to put forth countless hours teaching me IDL, supplying data, and giving council. In addition, I would also like to thank the other members of my master's committee, Courtenay Strong and Zhaoxia Pu, for setting aside their valuable time to critique this study.

Finally, I would like to thank my family and friends who loved, supported, and encouraged me throughout my graduate school career and thesis.

1. INTRODUCTION

1.1 The Stratospheric Polar Vortex

Over the next 100 years scientists predict CO₂ concentrations to nearly double to around 800 ppm. Vast amounts of research within the last decades have been conducted to understand how the atmosphere as a whole and its individual features might change amidst increased CO₂ levels. The particular interest of this study is the stratospheric polar vortex and how it may change in the future. The stratospheric polar vortex is the name for a region of strong westerlies that develop during winter over the high latitudes and that generally increase in strength with height. During summer, geopotential heights increase poleward causing an anti-cyclonic circulation to form according to the thermal wind relationship. As winter approaches, this height gradient reverses as high latitude regions receive low amounts of solar radiation. Easterly winds that were prevalent through summer now become westerly, marking the onset of the wintertime polar vortex. During the period that solar radiation becomes nearly absent, commonly called polar night, these westerly winds increase in intensity and eventually peak shortly after the winter solstice. In Figure 1 during winter, the stratospheric polar vortex can be seen pole ward of 30° and above 100 hPa in each hemisphere.

The stratospheric polar vortex also experiences strong variability during certain timeframes of the year. During summer, the polar stratosphere circulation remains largely undisturbed. However, as winter approaches and the polar vortex strengthens, the potential for its circulation to be disrupted also increases. Highlighted by Figure 2, it is

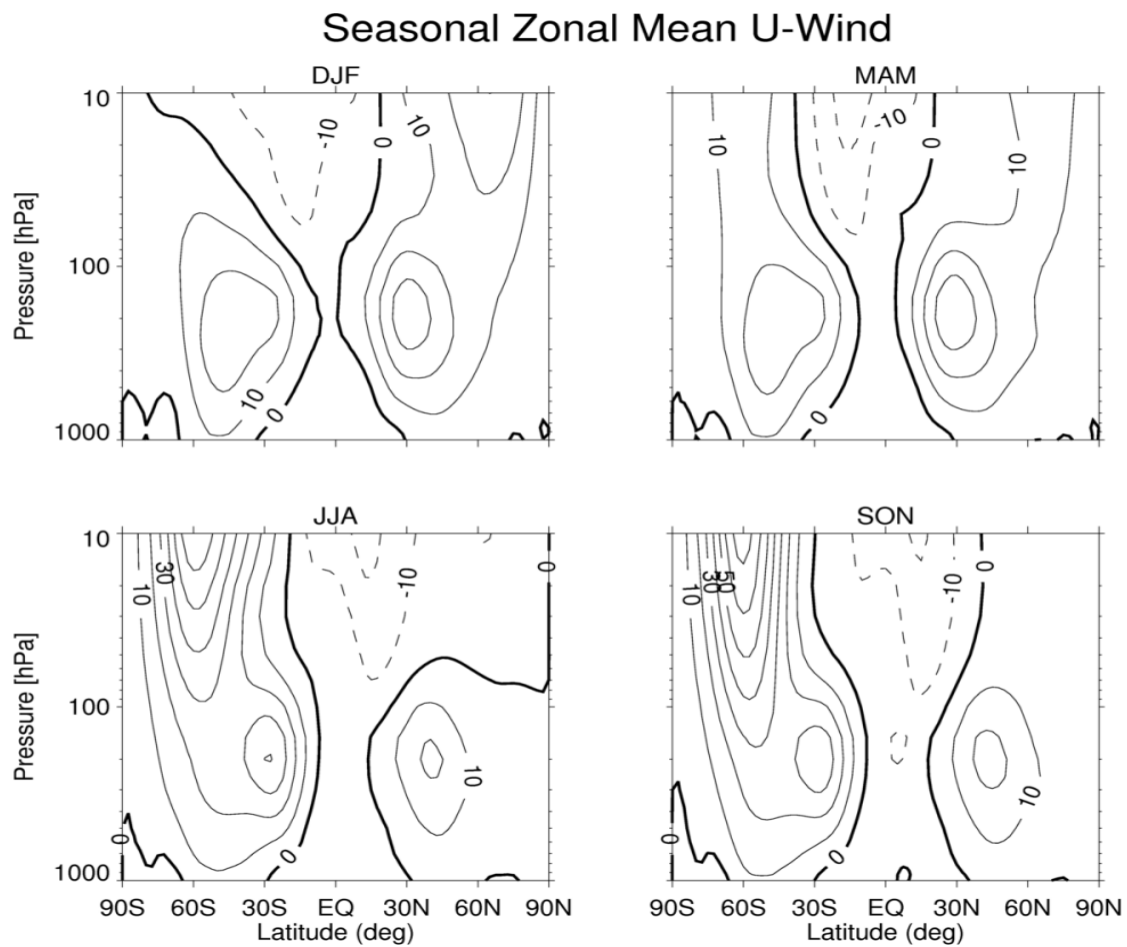


Figure 1. Seasonally averaged zonal-mean zonal wind (m/s) derived from NCEP-NCAR reanalysis (1948-2010). Log-pressure height coordinate on y-axis. Contours are every 10 m/s. Dashed lines are easterlies.

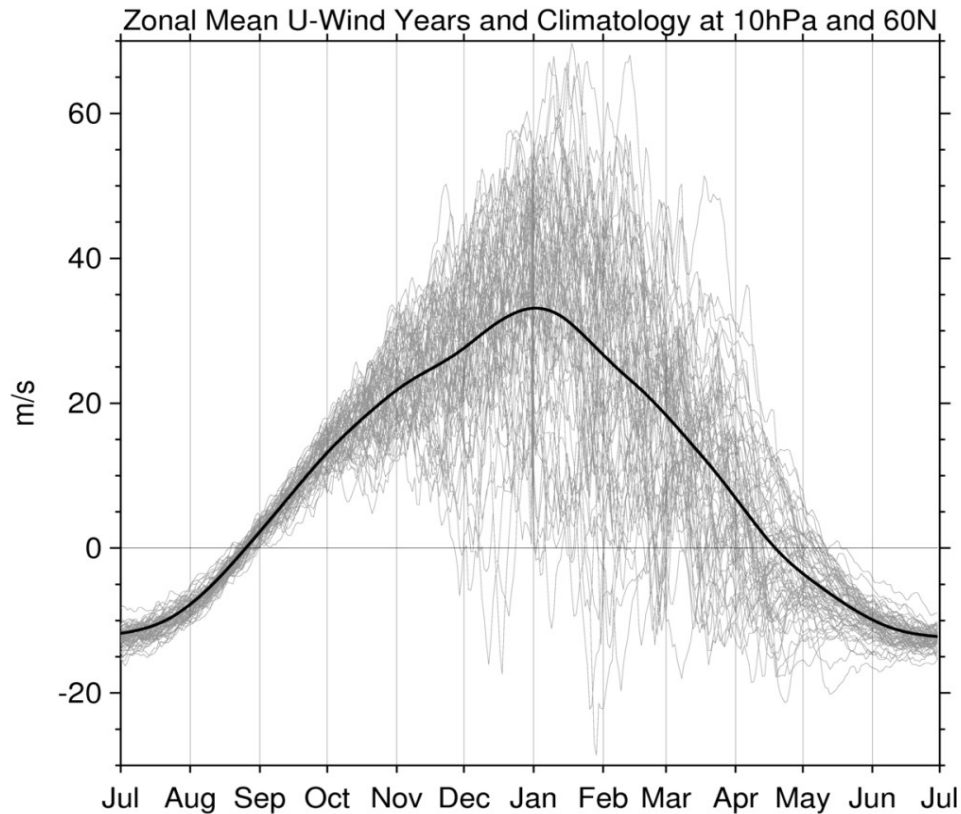


Figure 2. Light gray lines indicate individual years of zonal mean u-wind (m/s) derived from NCEP-NCAR reanalysis (1948-2010). Black line is daily reanalysis climatology smoothed by a Gaussian 45-day running mean.

clear that the Northern Hemispheric polar vortex undergoes the greatest variability through the middle and end of winter. During this time, the polar vortex winds can strengthen to twice the magnitude of climatology or can have a more easterly circulation than what is seen in the middle of summer.

Given that the polar vortex is prevalent throughout the high and mid-latitudes, it is the dominant boreal wintertime circulation feature in the stratosphere. Therefore, potential changes in its mean strength and/or variability over the next century may have important implications. For example, past research showed that the strength and variability of the polar vortex affect springtime polar ozone depletion (Anderson and

Knudsen, 2006). This is due to the formation of polar stratospheric clouds (PSCs) during winter under cold stratospheric conditions and the impact of the polar vortex on temperatures. Through PSCs, atmospheric chlorine is activated which destroys ozone when exposed to solar radiation. Since the presence of a stratospheric cold pool is essential for the depletion process, it is highly dependent on a strong and cold polar vortex.

Further motivation for investigating possible future changes in the structure of the polar vortex is the significant influence of the vortex on tropospheric weather (Baldwin and Dunkerton, 1999; Kolstad et al. 2010; Thompson and Wallace, 2000; Thompson et al. 2002; Black et al. 2006). For example, Baldwin and Dunkerton (1999) show stratospheric geopotential height anomalies associated with a cold (strong) or warm (weak) polar vortex propagate downward to the troposphere over a period of ~2-3 weeks, and significantly affect the Arctic Oscillation (AO) at the surface. As Figure 3 suggests, the two opposing polar vortex scenarios show significant differences in jet stream patterns and subsequent wintertime storm tracks, underlining the significance of the structure of the stratospheric polar vortex on tropospheric weather patterns.

Thompson et al. (2002) also studied the different surface impacts associated with a strong and a weak polar vortex. When examining surface temperatures associated with weak and strong vortex events, surface conditions are usually 1-2 K colder during a weak vortex event. Thompson et al. (2002) find that regions east of the Rocky Mountains in North America as well as parts of Europe and Asia experience twice as many cold air outbreaks per winter during weak vortex conditions as opposed to those winters of strong vortex conditions. Thompson et al. (2002) further find that the frequency difference of

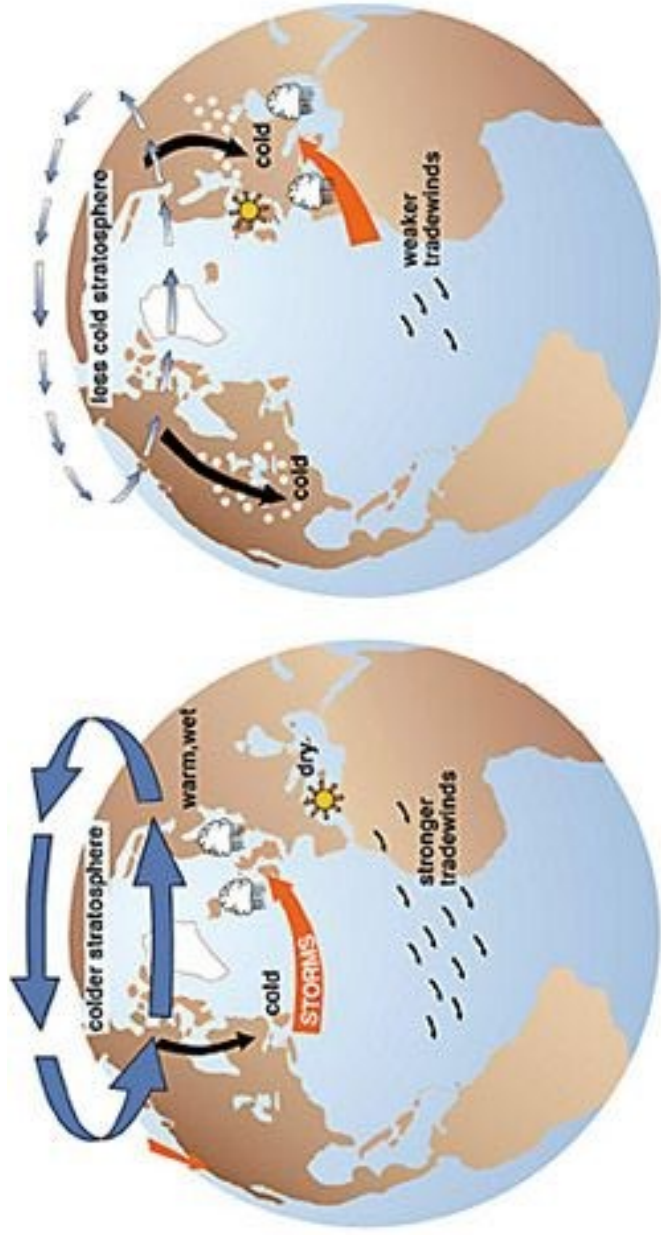


Figure 3. Schematic showing polar vortex modulation of tropospheric weather (Courtesy of John Wallace, University of Washington)

cold air outbreaks between weak and strong vortex events is as large as the frequency difference associated with the warm and cold phases of the El Niño-Southern Oscillation (ENSO).

There is also evidence that the onset timing of boreal spring is related to the polar vortex and its abrupt breakdown during this time of the year. Black et al. (2006) find during springtime anomalously weak or strong polar vortex conditions lead to high and mid-latitude geopotential anomalies at 1000 hPa. Since changes in the AO/NAO index are related to air temperature, sea ice and cloudiness, understanding the polar vortex during this season proves important (Wang and Key, 2003; Belchansky et al. 2004).

The works from Baldwin and Dunkerton (1999), Thompson et al. (2002), Black et al. (2006), and others show that conditions in the stratosphere impact tropospheric weather and climate and that this impact is significant. From a climate standpoint, this is important as it gives motivation for investigating potential future changes in the polar vortex.

The most dramatic events in the polar stratosphere occur when the polar vortex abruptly breaks down within the matter of a few days. These are so-called stratospheric sudden warming events (SSWs). These events are caused by planetary scale tropospheric waves propagating upward into the stratosphere (Andrews et al. 1987; Taguchi, 2003). When these waves break, they disrupt the circulation of the polar vortex. The combination of the disruption of the stratospheric cold pool, and the consequential enhanced subsiding air related to the Brewer-Dobson Circulation are responsible for the large and sudden warming that occurs during SSWs. Both warming and decreased zonal

wind in the polar stratosphere are attributes of SSWs and have been used to define them. Traditionally a threshold of westerly winds at 10 hPa becoming 0 meters per second (m/s) is used to define SSWs.

Since 1979, the average frequency of SSWs has been approximately 0.6 events/yr. However as the Earth's climate changes, it might be possible that the strength and/or variability of the polar vortex undergoes change as well. In particular, investigating the possibility of potential changes in SSW frequency is important for reasons mentioned above. However, this work can be based only on data from global climate models (GCMs) that can simulate Earth's climate system under current and future conditions. In order to build confidence in how well a GCM can simulate the stratospheric polar vortex and its potential changes under future climate, replicating the SSW frequency is a crucial requirement. Various past studies and also the present study are concerned with this question.

1.2 Literature Review and Objectives

Charlton et al. (2007) investigate six stratosphere-resolving GCMs and compare each model with the climatological strength of the vortex and the SSW frequency seen in NCEP-NCAR reanalysis. Charlton et al. find that only data from three of the six models are within one standard deviation of the winter (Nov-Apr) zonal mean zonal wind 10 hPa climatology seen in the reanalysis. This is important to note since the strength of the zonal wind and its seasonality is used to measure the polar vortex. For reasons more thoroughly discussed later, a model's ability to accurately replicate the average frequency of SSWs is highly contingent on the strength of the simulated polar vortex in each model. All in all, three models in Charlton et al. are unable to simulate the observed SSW

frequency compared with reanalysis and no model is able to replicate the monthly varying frequency of SSWs.

Measuring the dynamics involved in SSWs was also examined by Charlton et al. (2007). The goal of their study is to investigate how well models simulate the dynamics of SSWs as seen in reanalysis. The authors find that all six models investigated accurately reproduce the dynamical benchmarks in comparison to each other and to NCEP-NCAR reanalysis. Charlton et al. thus conclude that the lack of similarities in SSW frequency in each model is not because a model cannot reproduce the dynamics involved in each SSW. Instead, it is the dynamics that cause SSWs that are being produced more or less frequently compared to reanalysis.

Outside of dynamical reasoning, the World Meteorological Organization (WMO) defines SSWs as the zonal-mean zonal wind at 60°N at 10 hPa dropping to 0 m/s. Therefore, a model not being able to replicate SSW frequency could be related to the strength of the polar vortex because on average the zonal wind could be closer or farther from the 0 m/s threshold value. This means a weaker polar vortex, assuming the magnitude of polar vortex disruption does not change, will lead to a higher frequency of SSWs using the WMO absolute criterion. On the other hand, a stronger polar vortex is associated with the opposite behavior. One important goal of the present work is to find a more objective criterion than that of the WMO criterion, which is less sensitive to changes in the mean strength of the polar vortex.

McLandress and Shepherd (2009) used the Canadian Middle Atmosphere Model (CMAM) to examine changes in both past and future SSW frequency. Their model accurately reproduces past polar vortex zonal-wind zonal mean climatology as seen in

NCEP-NCAR reanalysis as well as past SSW annual frequency. Future projected changes in SSWs are determined by two criteria. The first is the absolute WMO criterion while the second is a relative criterion based on empirical orthogonal function (EOF) analysis, using the Northern Annular Mode (NAM). Reasoning for a second relative criterion is to accurately monitor polar vortex variability despite potential changes in stratospheric polar geopotential height climatology associated with climate change. McLandress and Shepherd (2009) justify the necessity for a relative criterion by their results that show when the absolute criterion is used, the frequency of SSWs increase while the relative criterion show no change. This is understandable considering that CMAM shows under climate change a climatologically weakened polar vortex even when SSW years were excluded. This weakened base state allows for the WMO criterion of 0 m/s to be more easily met. Given no significant change in SSWs in the NAM index, McLandress and Shepherd (2009) thus conclude that under increased CO₂ forcing, SSW frequency will remain unchanged amidst a weaker polar vortex if a relative criterion is used.

McLandress and Shepherd (2009) also examined SSW dynamics similar to those in Charlton et al. (2007). Overall, most benchmarks investigated by McLandress and Shepherd were similar to those found in NCEP-NCAR reanalysis. However, under climate change, when averaging future SSWs identified by either the NAM or WMO criterion, the average magnitude of SSWs decrease. Future wave forcing into the lower stratosphere also decreases (albeit at ~90% confidence level) when composites are made for the WMO criterion SSWs. This is of no surprise since the occurrence and magnitude of SSWs has been strongly tied to the amount of wave forcing from the troposphere. McLandress and Shepherd (2009) suggest a decrease in both SSW magnitude and wave

forcing is related to how an SSW is defined. According to the WMO criterion, a future weakening of the polar vortex will allow the 0 m/s threshold to include more events that are weaker in magnitude. This is highlighted further by a composite of future wave forcing for NAM SSWs that show a statistically insignificant increase; opposite of the same composite of WMO SSWs showing a decreased amount of future wave forcing. This future wave forcing difference illuminates a possible disadvantage of using an absolute SSW criterion to realistically grasp changing SSW dynamics amidst a changing climate. The above dynamical results by McLandress and Shepherd further prove the need for an improved SSW criterion that is more objective when examining SSWs under climate change. Not only might the absolute WMO criterion unrealistically change SSW frequency but also misrepresent SSW dynamics as proposed by McLandress and Shepherd.

Bell et al. (2010) examine the response of the Met Office HadSM3-L64 GCM under CO₂ forcings at preindustrial (control), two and four times preindustrial levels. Using the WMO criterion, Bell et al. (2010) show a near doubling of SSW frequency from the control run to the four times CO₂ simulation. Not only is annual SSW frequency investigated but also monthly annual frequency. Both two and four times CO₂ runs exhibit an increase in SSWs/yr in most months. The four times CO₂ run exhibit frequency increases throughout all winter months but particularly in early to mid-winter (November thru January).

As is evident in Bell et al., as CO₂ increases in each simulation so does SSW frequency. As is seen in Charlton et al. (2006) and McLandress and Shepherd (2009), any change in the frequency of WMO SSWs is primarily the result of a change in the strength

of the polar vortex. In order to address if the frequency change is due to the SSW criterion being more easily met due to a weaker polar vortex, the authors isolate zonal winds during non-SSW years from the two times preindustrial run and subtract zonal wind values from the control run. Bell et al. show that the polar vortex strength does not significantly change between these composites. This means that unlike in McLandress and Shepherd (2009), the increase in SSWs under increased CO₂ concentrations is not related to a weakened polar vortex but instead to an increase in polar vortex variability.

Bell et al. purposefully avoid the use of the NAM for identifying SSWs put forth by McLandress and Shepherd (2009). The premise of this omission is twofold. The future polar stratosphere geopotential height climatology used to base anomalies off is assumed by McLandress and Shepherd to be constant. Since the mean state of the stratosphere continually changes amidst climate change, the anomalies that are used to mark the onset of an SSW could in fact be changing. In addition, the geopotential height climatology used to base the NAM index off of excludes future SSWs. This approach is claimed to be inaccurate by Bell et al. as SSWs are a contributing component of the climatological mean state of the stratosphere. Bell et al. underline that continuing use of the WMO criterion is most useful due to the ability to measure the zonal-mean zonal winds which can infer tropospheric wave activity propagating into the stratosphere.

Mitchell et al. (2012) compare the output of three chemistry-climate models (CCMs) to ERA-40 reanalysis data in the simulation of the seasonality of meridional heat flux at 100 hPa, WMO derived SSW frequency and their average magnitude. Mitchell et al. show the magnitude of heat flux throughout the winter is less than that found in reanalysis. Furthermore, two out of three models investigated under represent ERA-40

annual SSW frequency while all three models replicated smaller SSW magnitudes than reanalysis. The latter two results are consistent with each other because if the models simulate less wave forcing into the polar stratosphere than is found in reanalysis, there will likely be a lower frequency of SSWs with weaker magnitudes when compared to reanalysis. In order to investigate SSW frequency under climate change, Mitchell et al. include seven other models from CCMVal-2 for an intercomparison of SSW trends. While the models show a wide range of increasing or decreasing trends, the multimodel mean had a statistically insignificant positive trend of ~ 0.1 SSWs/decade. This indicates that GCMs are not in full agreement as to the future projections of SSW frequency.

Consequently, this brings to light the need for other GCMs to either add or lower confidence in the above indeterminate trend. Not only is SSW frequency itself important but also why SSW events are in fact happening. As has been discussed, polar vortex strength, tropospheric wave energy into the stratosphere, and how SSWs are defined impact how the frequency of SSWs change in the future. This issue will be investigated in this study.

Finally, the reanalysis dataset that will be used in this study for analyzing the stratosphere only spans 64 years. Compo et al. (2011) derived a 20th century reanalysis (C20R) dataset from the surface to the middle stratosphere (10 hPa) using observed sea-level pressure (SLP) starting in 1871. This dataset could significantly expand the amount of observationally-based data that are currently available for the stratosphere. Therefore, it is of interest in this study to investigate whether the C20R accurately reproduces the polar stratosphere and if it can be used for stratospheric analysis.

In light of the findings by the above authors this study will set out to accomplish four main objectives:

- **Objective 1. Develop and analyze alternative methods for classifying SSW events**

As outlined by McLandress and Shepherd (2009), amidst a potential change in polar vortex strength, defining SSWs by the absolute WMO criterion could potentially make the 0 m/s threshold easier or more difficult to meet. The development of a more objective relative criterion could prove useful as it could be implemented in both a current, future, and changing stratospheric climate.

- **Objective 2. Investigate the SSW response of different climate forcing scenarios**

Since atmospheric CO₂ levels and SSTs over the next century are expected to increase, investigating a forced GCM simulations may shed new light on potential future changes of SSWs. The GCM simulations to be analyzed in this project have not been investigated in terms of their potential future changes in SSW frequency.

- **Objective 3. Inspect the response of SSW dynamics under climate forcing scenarios**

As highlighted by Charlton et al. (2007) and McLandress and Shepherd (2009), the principle cause of SSWs is the upward propagation of tropospheric wave energy. Not only should wave energy be quantified to

find potential changes amidst different forcing scenarios but also if the wave energy itself is making it into the vortex or is diverted equatorward.

- **Objective 4. Explore the reliability of the SLP derived C20R reanalysis dataset for potential SSW analysis**

Compo et al. (2011) undertook the creation of a 20th century reanalysis project derived from SLP data. This dataset spans up to 10 hPa and could potentially double the amount of reanalysis years for analyzing SSWs. By comparing this dataset with that of NCEP-NCAR reanalysis a potential conclusion could be reached for how accurate the polar vortex is in the C20R and if it should be used for SSW analysis.

2. DATA AND METHODS

2.1 Data

2.1.1 Observationally-Based Data

Observationally-based data in this study are taken from two sources: the NCEP-NCAR reanalysis (Kalnay et al. 1996) and the 20th century reanalysis V2 (C20R) (Compo et al. 2011). The NCEP-NCAR reanalysis has a vertical resolution of 17 levels between 1000 and 10 hPa and a horizontal resolution of 2.5° by 2.5° . Daily zonal-mean zonal wind and geopotential height data from 1948 to 2010 is utilized. Although other reanalysis datasets have a higher vertical and horizontal resolution, the NCEP-NCAR reanalysis dataset was selected due to the larger numbers of years used for our analysis. The C20R dataset has 24 vertical levels between 1000 hPa and 10 hPa with a horizontal resolution of 2° by 2° . Daily zonal-mean zonal wind and geopotential height data from 1871 to 2010 are utilized.

2.1.2 Model Data

The GCMs used include a standard (L24) and an enhanced (L48) version of the Geophysical Fluid Dynamics Laboratory (GFDL) Atmospheric Model v. 2.1 (AM2.1) (Delworth et al. 2006; Anderson et al. 2004). The standard version has 24 vertical levels up to 3 hPa while the enhanced model has a total of 48 levels. In the enhanced model, most additional levels add vertical resolution to the stratosphere from 100 hPa to 0.02 hPa (Figure 4). Horizontal resolution in both versions is 2° latitude by 2.5° longitude.

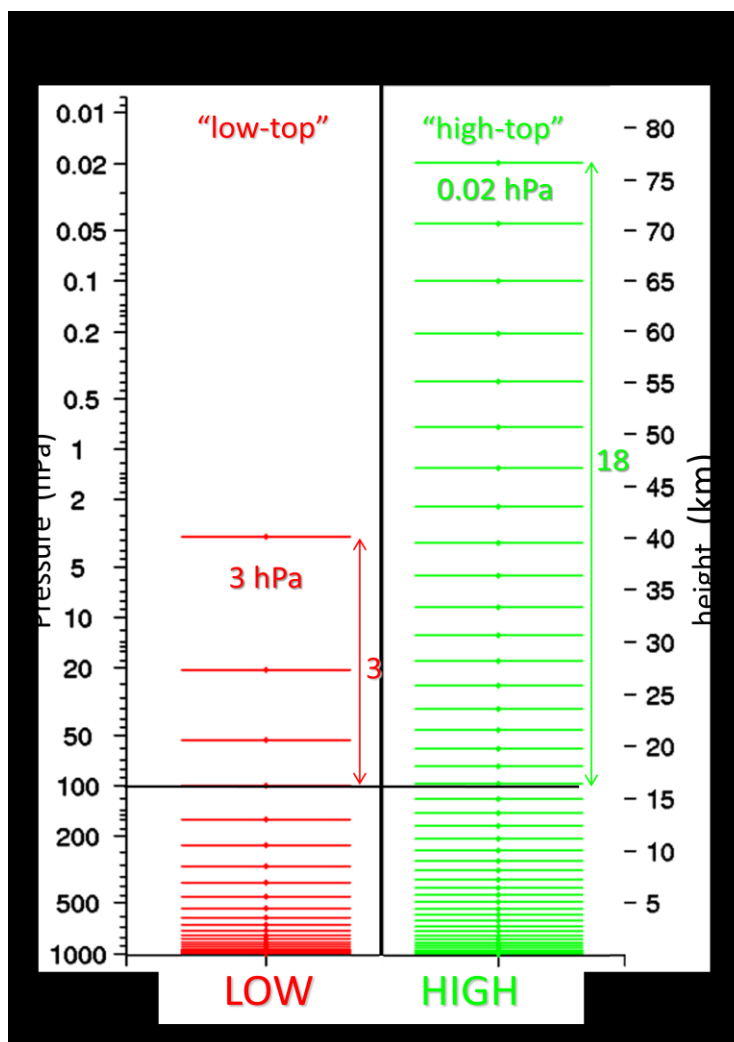


Figure 4. Schematic showing the position of vertical levels in the L24 and L48 models. Log-pressure height coordinate on left y-axis. Kilometer height coordinate on right y-axis.

Since the stratospheric polar vortex has a truly large structure and since it is mostly affected by planetary waves, the horizontal resolution in the GFDL GCMs should be able to accurately resolve this stratospheric phenomenon and its drivers.

The GFDL AM2.1 is forced by prescribed preindustrial concentrations of trace gases, aerosols, and SSTs. This preindustrial control run was made for the IPCC fourth assessment (AR4) with the coupled sister model of the AM2.1, called Climate Model v2.1 (CM2.1) (Delworth et al. 2006). The SSTs are derived from a preindustrial control

run carried out with the CM2.1. As described in Staten et al. (2011), a 10-year averaged timeframe is used from the CM2.1 to account for any SST variability that might occur. The control run of the AM2.1 is run in equilibrium for 2000 years to minimize the impacts of natural variability (see Table 1).

How the polar vortex changes amidst different forcing scenarios by changing CO₂ concentrations, SSTs, and a combination of the two is the primary focus of this study. Therefore, for CO₂ concentrations, three other forcing experiments with the AM2.1 are analyzed: half, two, and four times preindustrial concentrations. For SSTs, two other prescribed SST simulations are investigated that are also taken from CM 2.1. These two

Table 1: Concentration of CO₂, the corresponding years SSTs are taken from, and number of years each forced experiment in equilibrium is run.

| Simulation | CO ₂ | SSTs | Length (years) | |
|-------------------------|-----------------|------|----------------|------|
| | | | L24 | L48 |
| Control | 280 ppm | 1860 | 2300 | 2000 |
| CO₂ | | | | |
| 0.5xCO ₂ | 140 ppm | 1860 | 500 | 500 |
| 2xCO ₂ | 560 ppm | 1860 | 500 | 500 |
| 2xCO ₂ | 1120 ppm | 1860 | 500 | 900 |
| SST | | | | |
| 2050 | 280 ppm | 2050 | 500 | 500 |
| 2100 | 280 ppm | 2100 | 500 | 500 |
| Combined | | | | |
| 2xCO ₂ _2100 | 560 ppm | 2100 | 500 | 500 |

future SST experiments, taken from projected SST levels at 2050 and 2100, are derived from CM2.1 using prescribed greenhouse forcings for the A1B scenario from the AR4. Also, one combined forcing scenario is analyzed with two times preindustrial CO₂ concentrations and projected SST levels from the A1B scenario at 2100.

2.2 Methods

2.2.1 NAM Index

For each experiment, a precalculated daily NAM index is utilized. These calculations are based on a 900 year long dataset of zonally averaged geopotential heights at 10 hPa northward of 20°N. The first 450 years of this dataset are taken from the control run, and the second 450 years are taken from the forced experiment under consideration. The anomalies for each half of the dataset are derived relative to their own respective climatology. Then, a standard EOF analysis is carried out on the combined 900 year long dataset. We then compare the resulting EOF index for the second 450 years (belonging to the forced simulation) as it relates to the first 450 years (belonging to the control run).

While the NAM method found in this study and the one found in McLandress and Shepherd (2009) are similar, there are differences in how the NAM SSWs are identified. The differences are in the models investigated as well as the criteria used to identify SSWs. In McLandress and Shepherd, a transient climate simulation is analyzed whereas the current study compares two equilibrium climate simulations. In order to gauge potential polar stratospheric changes amidst climate change both a past and a future climate state must be used to calculate the EOF. Since the model used by McLandress and Shepherd is transient, the EOF pattern calculated over the past and future climate

cannot fully resolve changes in polar vortex variability that might possibly exist between these two climate states. Due to our model being run in equilibrium, every year is contributing to the climatology used to construct the EOF and thus we believe it will better represent potential future changes of SSWs. The second difference between the NAM method in this study and the one by McLandress and Shepherd is the SSW threshold. The authors chose a -2.5 NAM index threshold whereas this study counts SSWs as dropping to a value of less than or equal to -3.

2.2.2 Eliassen-Palm Flux

Precalculated data is of Eliassen-Palm (EP) Flux analysis and its divergence is employed to quantify the upward propagation of tropospheric wave energy over winter months and its potential convergence in the polar stratosphere. EP-flux analysis is used to calculate the effect of meridional heat transports and meridional momentum transports by eddies on the zonal-mean zonal wind. The meridional momentum and heat fluxes are represented by respective v and z vectors on the meridional plane. The acceleration (deceleration) found the combined momentum and heat flux vector (\mathbf{F}) can be used to calculate the divergence (convergence) in a given area. The equation given below is an approximation of the effect the divergence term has on the zonal-mean zonal wind acceleration:

$$\frac{\partial \bar{u}}{\partial t} \propto \nabla \cdot \mathbf{F} . \quad (1)$$

In Equation 1, when the divergence term is negative, it results in convergence which brings a deceleration to the zonal-mean zonal wind. To measure the amount of EP-flux divergence in the polar stratosphere, the mean of an area-weighted region is calculated between 50°N to 90°N and 100 hPa to 10 hPa. Associated units for EP-flux divergence

are $m \cdot s^{-1} \cdot day^{-1}$. Also, to better visualize EP-fluxes entering the stratosphere, vectors above 100 hPa are multiplied by a factor of 10.

To quantify the change in amount of upward propagating wave energy that is entering the stratosphere between forcing scenarios, the upward EP-flux vectors are averaged over an area at 100 hPa northward of $50^{\circ}N$. The change in convergence between forcing scenarios is also quantified by the average of convergence values between 100 and 10 hPa and northward of $50^{\circ}N$. These two areas are shown in Figure 5.

2.3 Approaches Used To Define SSWs

Prior to discussing our methods for identifying SSWs, two potential issues arise. The first is a possible change in the mean strength of the vortex, potentially allowing

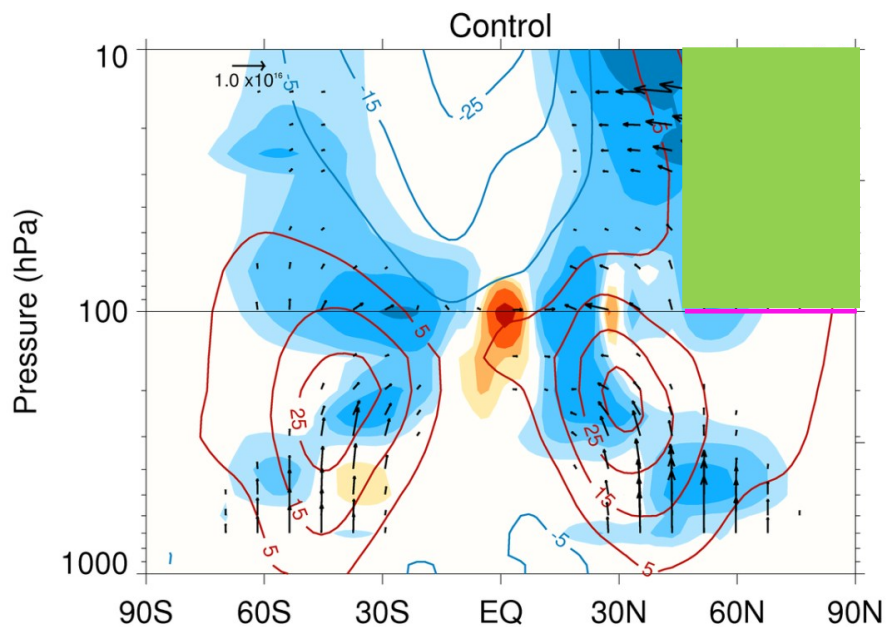


Figure 5. EP-Flux vectors, divergence, and zonal-wind. Y-axis is log-pressure height with latitude on x-axis. Eliassen-Palm flux arrows with reference arrows for the control are 1×10^{16} (kg/s^2). Non-filled colored contours are zonal-mean zonal wind values (m/s). Filled colored contours are the convergence (blue) and divergence (red) values (m/s/day). Area above 100 hPa horizontal line is multiplied by a factor of 10 for stratospheric analysis. Areas that calculate the upward propagating wave energy (pink line) and the convergence of wave energy in the polar vortex (light green box).

more or less SSWs to be counted. As mentioned earlier, an SSW event is traditionally classified when the zonal-mean zonal wind speed at 10 hPa and 60°N decreases to 0 m/s. This approach, brought forth by the WMO, has been criticized by McLandress and Shepherd (2009) and other authors. The authors argue that if the mean strength of the polar vortex changes under climate change then an absolute threshold of 0 m/s will allow the zonal-mean zonal wind to either be easier or more difficult to be met. This will cause the SSW frequency results in future climate scenarios to be biased. The misrepresentation of SSW frequency may potentially be resolved by developing a SSW criterion that is more objective and less affected by changes in the mean strength of the polar vortex.

The second issue is determining whether a future climatological change in the strength of the polar vortex is either due to a change in the strength of the polar vortex itself or a change in the frequency of SSWs, which would in turn also impact the mean strength of the polar vortex. To address this issue, both McLandress and Shepherd (2009) and Bell et al. (2010) take meridional cross-sections of the average zonal-mean zonal wind in non-SSW winters in a present and future climate to investigate if the mean strength of the polar vortex changes apart from SSW activity. While separating SSW years from non-SSW years is straightforward, the method is still ambiguous. For example, if the future mean strength of the polar vortex in non-SSW winters is weaker, is the mean strength of the polar vortex itself weaker or is it because the stratosphere experiences more “SSW” events that only drop to 1 m/s, thus not being counted by the traditional WMO SSW criterion? The converse also could be true that a stronger non-SSW winter vortex could mean less 1 m/s “SSWs” or that there is a stronger vortex causing less events to reach the 0 m/s threshold. Developing different SSW criteria

may potentially shed more light on the question whether the mean strength of the polar vortex itself is changing or if it can be attributed to a potential change in SSW frequency.

The two SSW criteria mentioned in McLandress and Shepherd (2009) are the WMO and the NAM criteria. As discussed earlier the NAM method is employed by the authors as an alternative to the WMO criterion. McLandress and Shepherd used the NAM index at 10 hPa to identify an SSW when the index dropped to -2.5. However, whether identifying SSWs by the zonal-mean zonal wind at 0 m/s or the NAM index at -2.5, both methods have a level of ambiguity to them. In light of this, we investigate in the present study different alternative criteria to identify SSWs through both the zonal-mean zonal winds at 60°N and 10 hPa and the 10 hPa NAM index. This is in hopes to find a criterion that is less dependent on the climatological strength of the vortex than the WMO criterion for identifying break downs of the polar vortex. In the following section we discuss criteria that are implemented in this study to shed further light on SSWs, potential change in frequency, and their cause amidst different forcing scenarios. All criteria except the NAM criterion are based on the zonal-mean zonal wind at 60°N and 10 hPa. The control run described in both the Magnitude and Kinetic criteria when investigating future forcing scenarios is NCEP-NCAR reanalysis data. Brackets denote zonal-mean values and overbars represent time averaged values.

2.3.1 WMO Criterion

This is the traditional WMO criterion. An SSW is defined when zonal-mean zonal wind falls to or below a threshold of 0 m/s, i.e.,

$$[U]_{\text{Threshold}} = 0 \text{ m/s.} \quad (2)$$

Zonal wind values that reach this threshold after the initial SSW event will not be counted until 50 days after the event. This allotted time is to avoid double counting the same event due to a significantly weakened vortex after an SSW event. The timeframe of 50 days was chosen as the value that was least sensitive to changing the final SSW count in the reanalysis data. This value was selected based on evaluating a range of different timeframes from 20 through 80 days.

2.3.2 Magnitude Criterion

The Magnitude criterion is a zonal-mean zonal wind adjusted threshold to account for a potential future change in the mean strength of the vortex. Mathematically, the criterion can be written as

$$[\bar{U}]_{\text{Threshold}} = [\bar{U}]_{\text{Experiment}} - [\bar{U}]_{\text{Control}}. \quad (3)$$

The daily zonal-mean zonal wind climatology of the control run is subtracted from the daily wind climatology of the forcing experiment. By doing this we account for any potential change in the mean strength of the polar vortex by making that difference on a given day the new threshold the zonal-mean zonal wind has to drop to. For example, if the mean zonal-mean zonal wind in the forcing experiment is 5 m/s stronger on January 15th than the wind in the control run then the threshold the zonal-mean zonal wind has to reach is only 5 m/s and not 0 m/s as in the traditional WMO approach. The opposite is also true: If the control run wind climatology is stronger than the experiment then the criterion threshold will be below 0 m/s. Once an SSW event occurs, this criterion will not search for another SSW for 50 days.

2.3.3 Kinetic Criterion

Similar to the Magnitude criterion, the Kinetic criterion is based on the difference of the zonal-mean zonal wind daily climatology values between experiments:

$$[U]^2_{Threshold} = [\bar{U}]^2_{Experiment} - [\bar{U}]^2_{Control} \quad (4)$$

The primary difference is that the daily zonal wind values are squared. This is to look at the polar vortex through an energetic perspective in terms of required changes in kinetic energy. The kinetic energy equation

$$E_{Kinetic} = \frac{1}{2}m(U^2 + V^2) \quad (5)$$

can be simplified by assuming the quantity of mass is constant. By doing this,

$$E_{Kinetic} \propto (U^2 + V^2) \quad (6)$$

kinetic energy is proportional to the sum of the squared values of U and V . However since this is the zonal-mean zonal wind flow at a given location we can also assume that v is zero. Therefore the squared U value of the wind's velocity is approximately proportional to the total amount of kinetic energy:

$$E_{Kinetic} \propto U^2. \quad (7)$$

As reflected in equation 4, the threshold is no longer the difference of the daily zonal-mean zonal wind climatologies for each experiment but rather the difference in the climatological daily kinetic energy values. The zonal-mean zonal wind values for each winter are also squared. An SSW event is counted when the kinetic energy of the polar vortex drops to the kinetic energy threshold. For example, if the climatological kinetic energy on January 15th for the forcing experiment is $900 \frac{\text{J}}{\text{kg}}$ ($U_e = 30 \frac{\text{m}}{\text{s}}$) and for the control run is $625 \frac{\text{J}}{\text{kg}}$ ($U_e = 25 \frac{\text{m}}{\text{s}}$), then the polar vortex would have to decrease in

kinetic energy to $275 \frac{\text{J}}{\text{kg}}$, or wind to 16.6 m/s, to be considered as an SSW event. Like the WMO and Magnitude criteria, once an SSW event occurs, this criterion will not search for another SSW for 50 days.

2.3.4 Drop Criterion

The Drop criterion is different from the previous SSW criteria because it is not tied to the daily mean strength of the polar vortex. The concept behind the Drop criterion is the following: if the zonal-mean zonal wind drops by more than 25 m/s in less than or equal to 7 days it is counted as an SSW event, i.e.,

$$\text{IF: } \Delta[U] \geq 25 \text{ m/s and } \tau \leq 7 \text{ days.} \quad (8)$$

This criterion introduces a temporal aspect by looking at a “sudden” breakdown of the polar vortex. What is also unique to the Drop criterion is that there is no 50 day lag before SSWs can be counted again. The Drop criterion breaks away from the traditional WMO standard for a lag time and instead looks again for SSWs once the vortex has re-strengthened.

The selection of a 25 m/s drop to occur within a week timeframe was derived from a composite image of zonal-mean zonal winds before, during, and after all WMO SSWs that occurred in the reanalysis data. In Figure 6, the region of uninterrupted drop is ~ 25 m/s and takes approximately one week to reach.

2.3.5 Kinetic Drop Criterion

The Kinetic Drop criterion has a similar framework as the Drop criterion. It looks for a drop in kinetic energy greater or equal to $1250 \frac{\text{J}}{\text{kg}}$ within 7 days. This value is

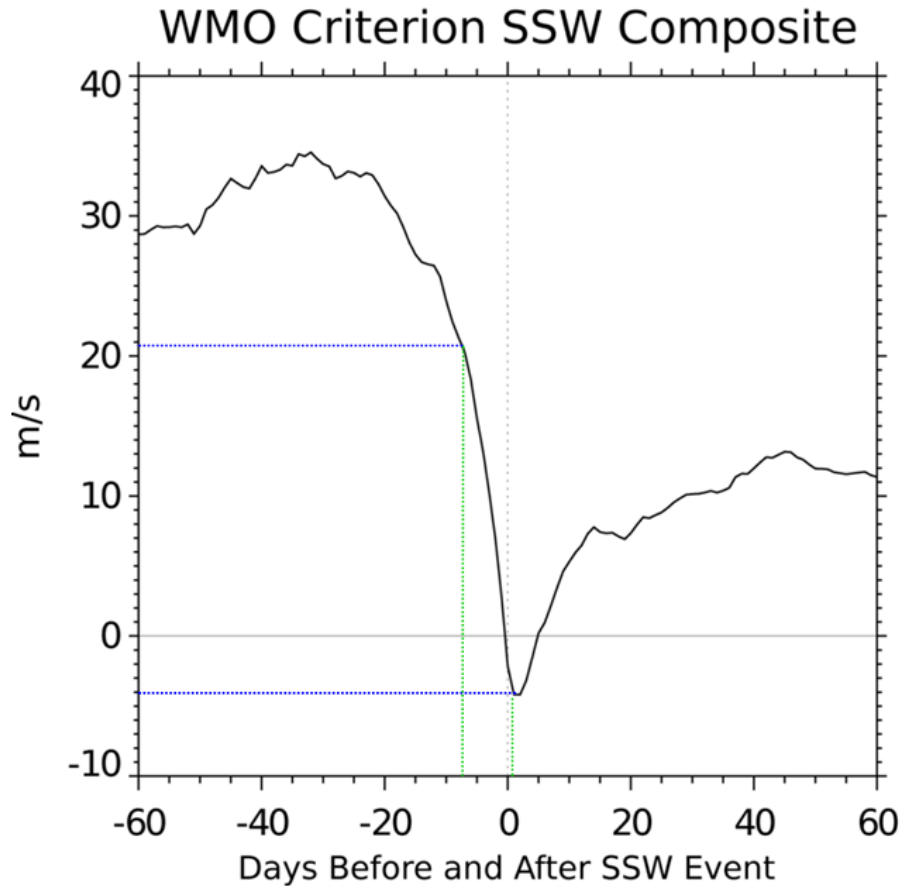


Figure 6. Composite of zonal-mean zonal wind at 60°N and 10 hPa for 60 days before and after 35 WMO criterion SSW events. Data from NCEP-NCAR reanalysis (1948-2010).

derived from twice the squared value of the 25 m/s drop looked for in the Drop criterion, i.e.,

$$\text{IF: } \Delta[U]_{\text{Threshold}}^2 \geq 2 \times (25 \text{ m/s})^2 \text{ and } \tau \leq 7 \text{ days.} \quad (9)$$

Like the Kinetic criterion, the zonal-mean zonal wind is converted to kinetic energy. Due to an overrepresentation of SSW events when looking for a drop of $625 \frac{\text{J}}{\text{kg}}$ (the squared value of the Drop criterion threshold), we somewhat arbitrarily multiplied the threshold by two to make the threshold more difficult to break. Once an SSW event

occurs, the criterion looks for a rebounding in kinetic energy before another SSW event can be counted.

2.3.6 NAM Criterion

As discussed earlier, if the NAM index drops to or below a value of -3, it will be counted as an SSW event. Once the value of -3 occurs, the criterion will not look for another SSW event for 50 days following an event.

2.4 March SSW Criterion

Stratospheric warming events that occur in March have to pass through an additional criterion in order to be counted as an SSW. This extra criterion is to ensure that an SSW criterion is not falsely counting SFWs. What has traditionally been used in the WMO criterion to separate a March SSW from a SFW event has been when zonal-mean zonal winds are above the WMO threshold of 0 m/s for at least 10 consecutive days. This March criterion is extended to the other criteria by looking for the polar vortex to be above their given threshold for a consecutive 10 days. For the Drop and Kinetic Drop criterion a zonal wind value above 0 m/s for 10 days is counted as an SSW event.

2.5 Testing for Statistical Significance

The following equation is taken from Wilks (2006):

$$Z = \frac{\bar{x}_1 - \bar{x}_2}{\left[\left(\frac{1}{n_1} + \frac{1}{n_2} \right) \left\{ \frac{(n_1 - 1)s_1^2 + (n_2 - 1)s_2^2}{n_1 + n_2 - 2} \right\} \right]^{1/2}} \cdot \quad (10)$$

Equation 10 will be used to test if there is a statistical significance between two mean SSW frequencies from different datasets. Whether investigating the SSW frequency annually or for individual months, both timeframes will have a binomial distribution

because we look for whether a given month or year has at least one SSW or not. Due to the large sample size of each model simulation we assume, due to the Central Limit Theorem, that each mean SSW frequency has a Gaussian distribution. Due to this, we can implement equation 10. The variance for each time series because of the large sample size is the same variance that would be used to find the statistical significant of a binomial distribution.

3. ANALYSIS

3.1 Reanalysis and Model Control Runs

3.1.1 Zonal-Mean Zonal Wind Comparison

We start our analysis by comparing the zonal-mean zonal wind between the reanalysis data and data from both the L24 and L48 versions of the GFDL AM2.1 model. This is to investigate how accurately the models simulate the polar stratosphere during boreal winter. In Figure 7 average zonal-mean zonal wind from December through February (DJF) for the reanalysis data and the L48 model data are compared. The L48 control run shows slightly stronger winds particularly above 20 hPa and north of 55°N. Overall, however, the L48 model is able to adequately replicate the overall spatial structure and magnitude of the meridional field zonal-mean zonal wind found in the reanalysis data. In Figure 8, the L24 model DJF zonal-mean zonal winds are compared to the L48 model zonal winds. It is clear that the L24 model has significantly stronger winds above 50 hPa. This strong wind bias can be primarily attributed to the lower vertical resolution above 100 hPa in the L24 model. As a result, the polar vortex in the L24 is ~12 m/s stronger at 10 hPa and up to ~20 m/s stronger at 4 hPa.

3.1.2 Zonal-Mean Zonal Wind Climatology

We also compare the zonal-mean zonal wind at 60°N and 10 hPa in the reanalysis and model data. This is the same latitude and height location for the zonal wind that will

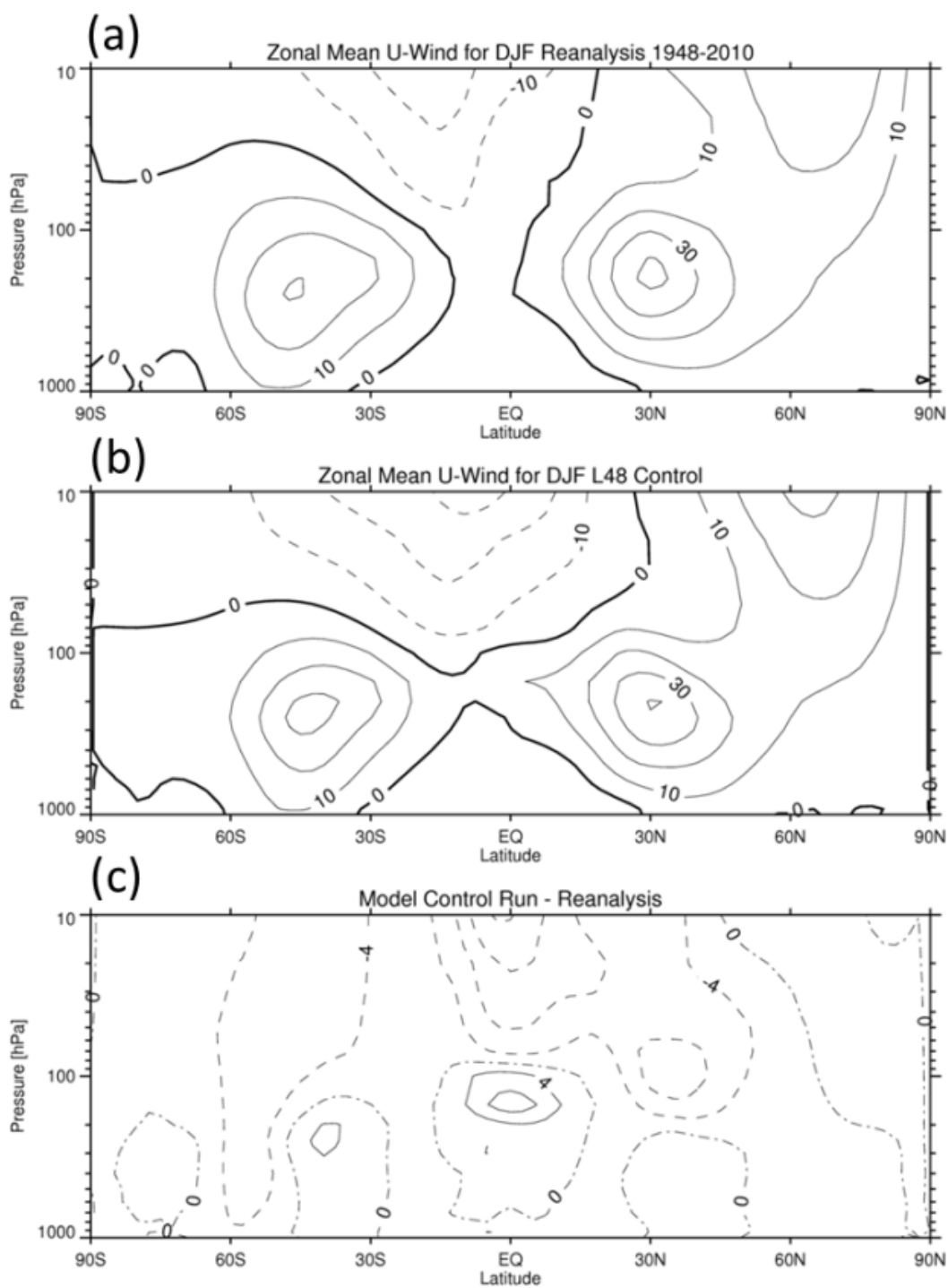


Figure 7. Zonal mean u-wind (m/s) during DJF. Y-axis is log-pressure height. (a) NCEP-NCAR reanalysis (1948-2010), (b) L48 model control run, and (c) is the difference (L48 - reanalysis). Contour interval is 10 m/s in (a) and (b) and 4 m/s in (c). Negative contours are dashed.

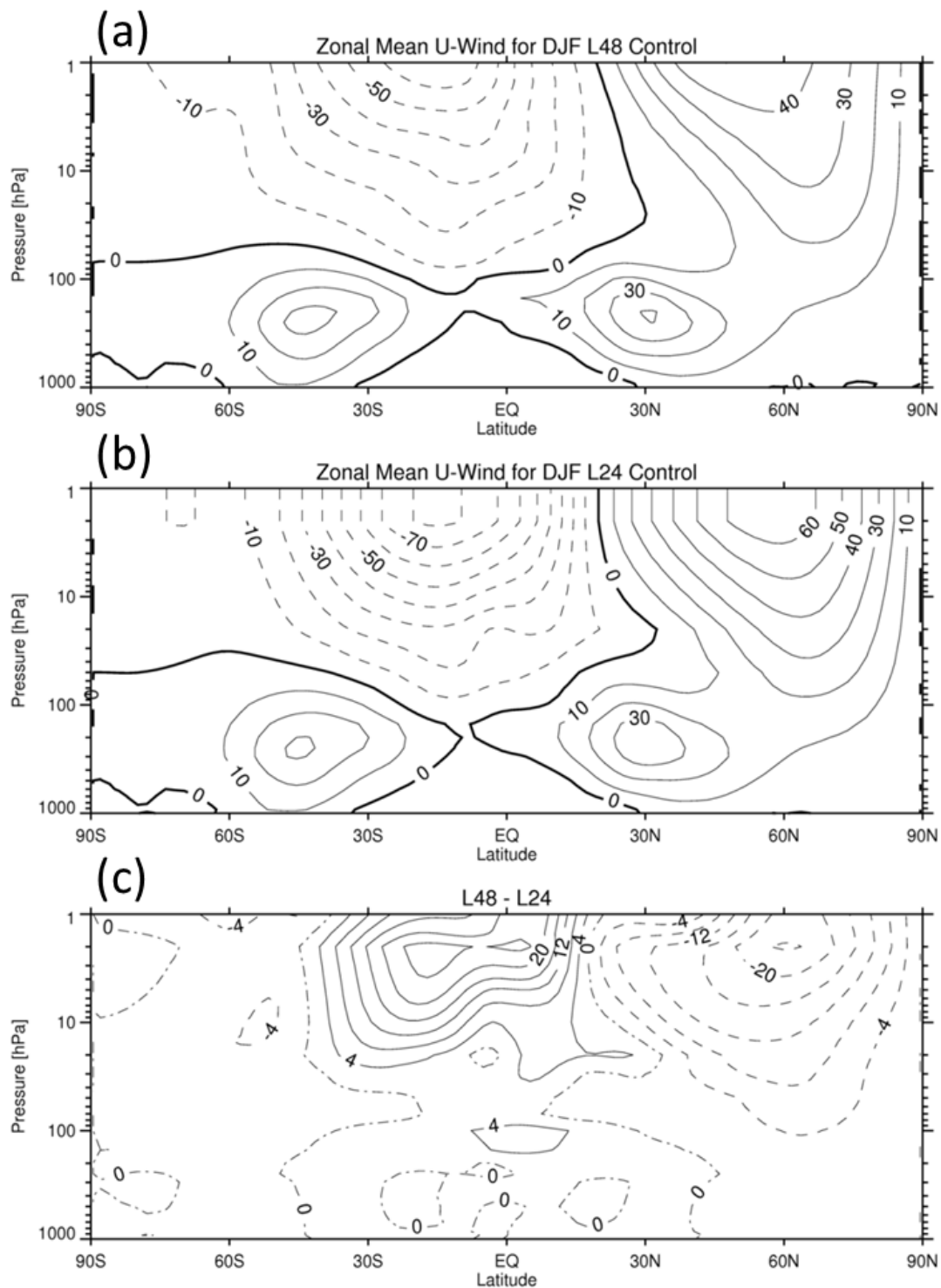


Figure 8. Model comparison between DJF zonal-mean u-wind (m/s) high-top and low-top control runs. (a) L48. (b) L24. (c) L24 run subtracted from L48 run. y-axis is log-pressure height. Contour interval 10m/s for (a), (b), 4 m/s interval for (c) Dashed lines represent easterlies

be used to identify SSWs. Figure 9 shows the daily climatological seasonal cycle zonal-mean zonal wind for the reanalysis, the L48, and the L24 data. In boreal summer, easterly winds are stronger in the reanalysis data and become westerly later in August than found in both the L24 and the L48 models. With the exception of early winter and spring, the reanalysis polar vortex is slightly weaker than the L48 for DJF. The L24 model, as was evident in Figure 8 for DJF, has a significantly stronger polar vortex throughout all winter months.

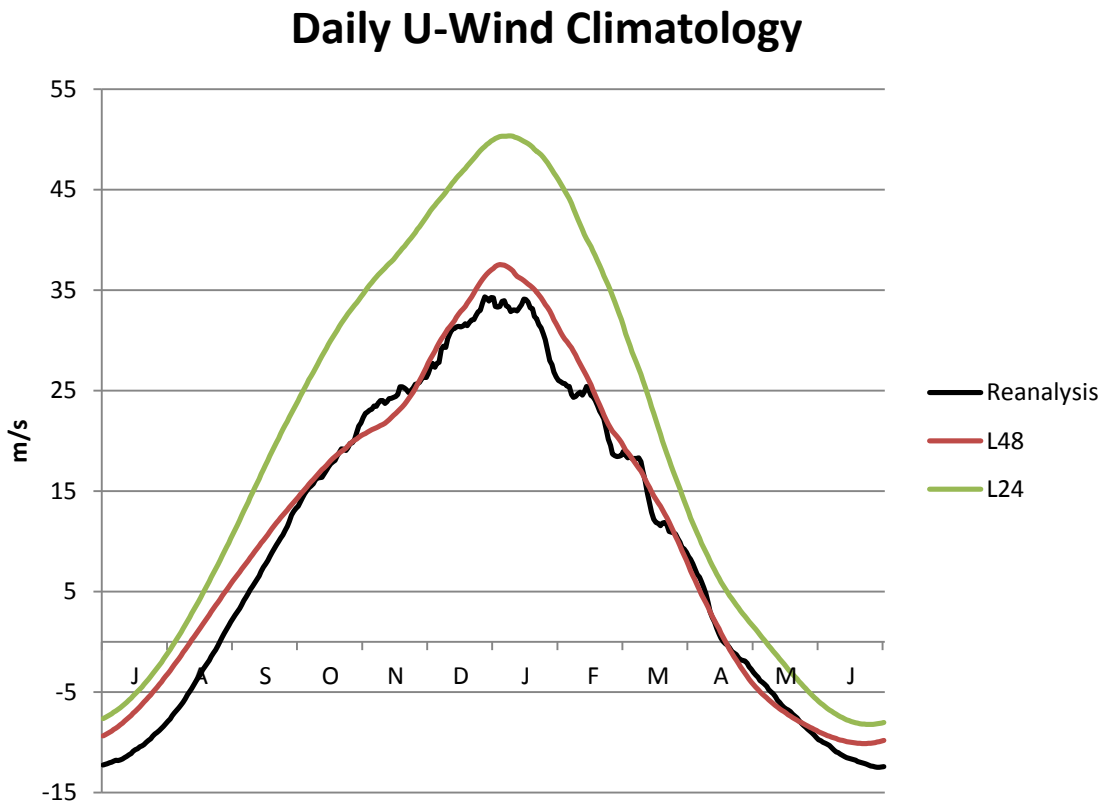


Figure 9. Zonal mean u-wind daily climatology at 10 hPa and 60N.

3.1.3 Mean Seasonal Variability

The daily mean standard deviation for the zonal-mean zonal wind at 60°N and 10 hPa is compared for the same three time series (Figure 10). For early to mid-winter, variability is highest in the reanalysis data and lowest in the L24 model. By mid-winter the L48 has a similar amount of variability as the reanalysis data and has a greater amount moving into February and early March. Only in late winter and early spring do the reanalysis, the L48, and the L24 model have a similar variability.

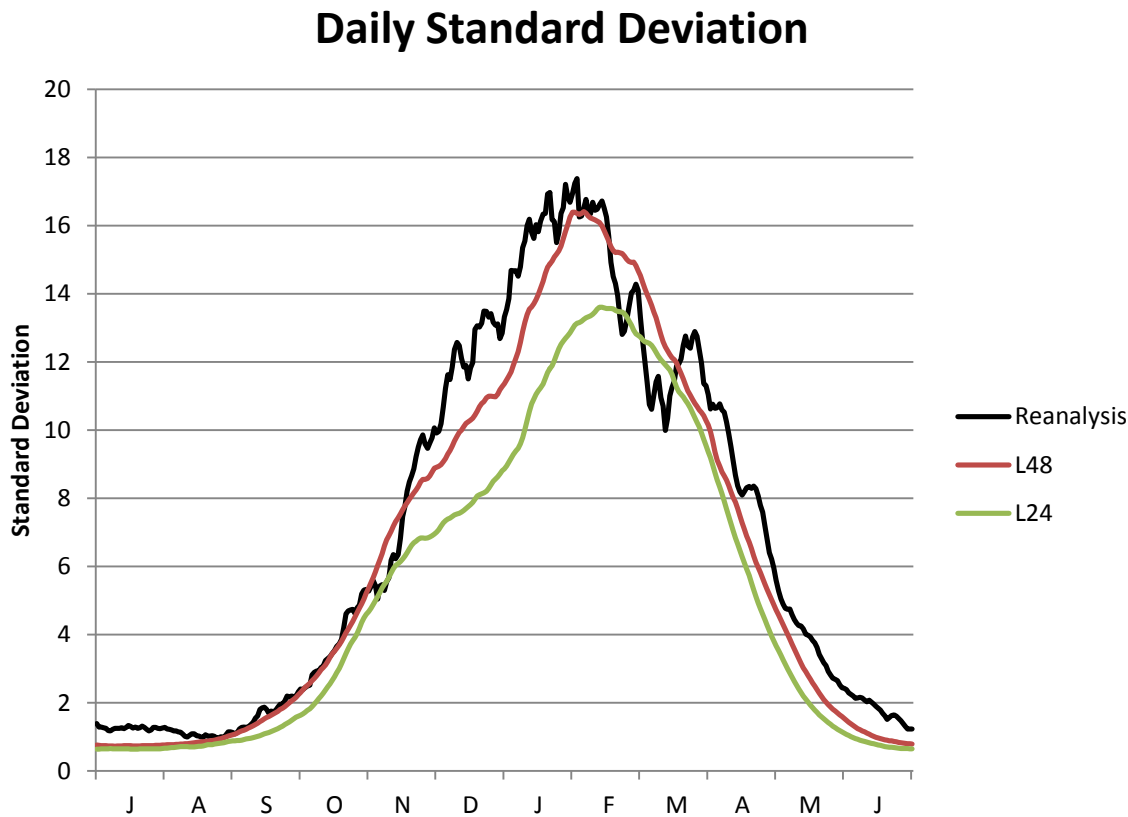


Figure 10. Daily mean standard deviation for the zonal-mean zonal wind at 60°N and 10 hPa for July thru June.

3.2 SSW Annual Frequency Summaries

The annual frequency of SSWs across each model and criteria is investigated in Figure 11. The reanalysis annual frequency for the first three criteria is unchanged based on the reanalysis being both the control and experimental run for the Magnitude and Kinetic criterion. The WMO criterion shows a similar annual frequency between the reanalysis and the L48 data. This can be attributed to a similar zonal-mean zonal wind climatology (Figure 9) and similar winter variability (Figure 10). The L24 model however is significantly lower in SSW frequency. As discussed earlier this is likely attributed to the significantly stronger polar vortex that makes reaching the 0 m/s threshold more difficult. Despite the SSW threshold adjusting for the difference in u-wind climatology in the Magnitude criterion, the L24 model is still significantly lower in SSW frequency than reanalysis while the L48 model remains similar to the reanalysis frequency. The Kinetic criterion reveals that both models, especially the L24, have a higher frequency than the reanalysis data. For both models, having a winter-mean polar vortex that is stronger than reanalysis allows for the kinetic energy threshold to be more easily met. The Drop criterion also shows a significant annual frequency increase in the L48 compared to the reanalysis while the L24 has a significantly lower annual frequency. The decrease seen in the L24 model can reflect the lower variability for the first half of winter as seen in Figure 10. Of interest, though, is the statistically significant increase in SSW frequency in the L48 model considering the variability is similar to the reanalysis data throughout winter. This result could illuminate the possibility that the SSWs being produced in the model are more “sudden” than what is seen in reanalysis. The Kinetic

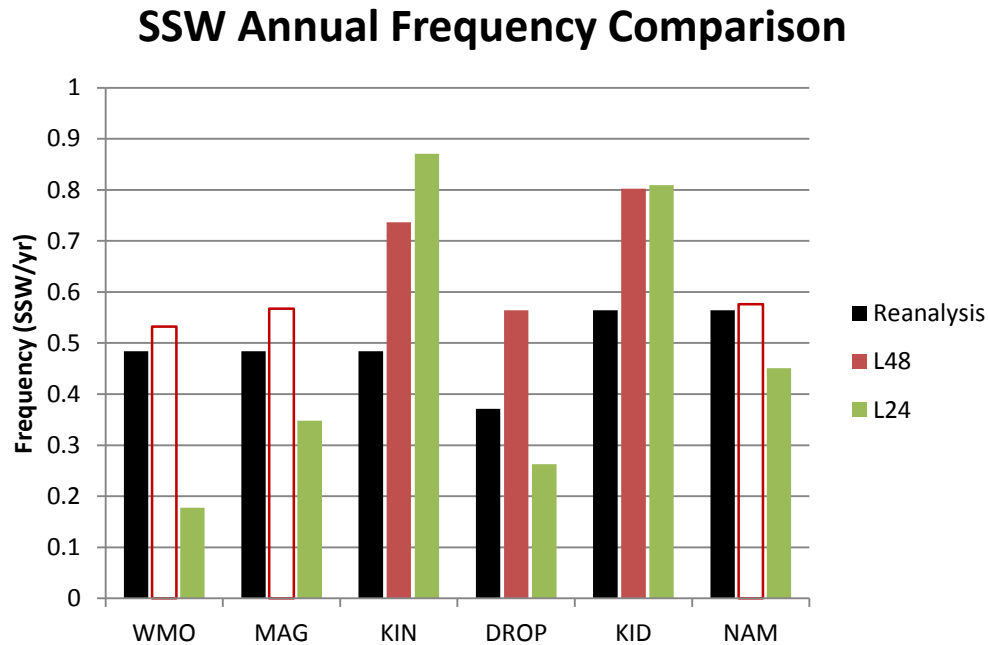


Figure 11. SSW frequency using the all criteria. Data included are NCEP-NCAR reanalysis, L24 and L48 model control run. Filled boxes indicate a 95% statistically significant difference from the reanalysis.

Drop criterion has one of the highest frequencies out of all the criteria and both the L48 and L24 model have a significantly higher frequency than reanalysis. Like the Kinetic criterion, the Kinetic Drop criterion overproduces SSWs likely due to a combination of strong winds and variability. The NAM criterion has virtually the same frequency between the reanalysis and L48 model. The L24 model, however, has a significantly lower SSW annual frequency. Although the NAM by definition is standardized, the distribution is perhaps not perfectly Gaussian and thus a -3 threshold could have less “events” than is expected. All in all, the L48 model throughout all criteria is either similar or greater in annual frequency than the reanalysis. The L24 model in every criterion has a lower annual frequency than reanalysis except for the criterion involving kinetic energy.

This is likely the result of the criteria based on kinetic energy counting SSWs more easily when there is a stronger polar vortex which makes them less reliable.

3.3 Monthly SSW Frequency Response

We now look at the monthly SSW frequency response using the WMO criterion. When identifying SSWs by the WMO criterion, Figure 12 reflects the annual frequency results shown in Figure 11: monthly SSW frequency between the reanalysis and L48 model control run are similar (except for January) and the L24 model control run SSWs are non-existent in early winter and nearly absent until late winter. As mentioned earlier, much lower frequency could potentially be attributed to the stronger polar vortex and lower variability found in the L24 model relative to the polar vortex found in the L48 and reanalysis data. To investigate whether SSW frequency using the WMO criterion is potentially affected by the mean strength of the polar vortex and to look more generally

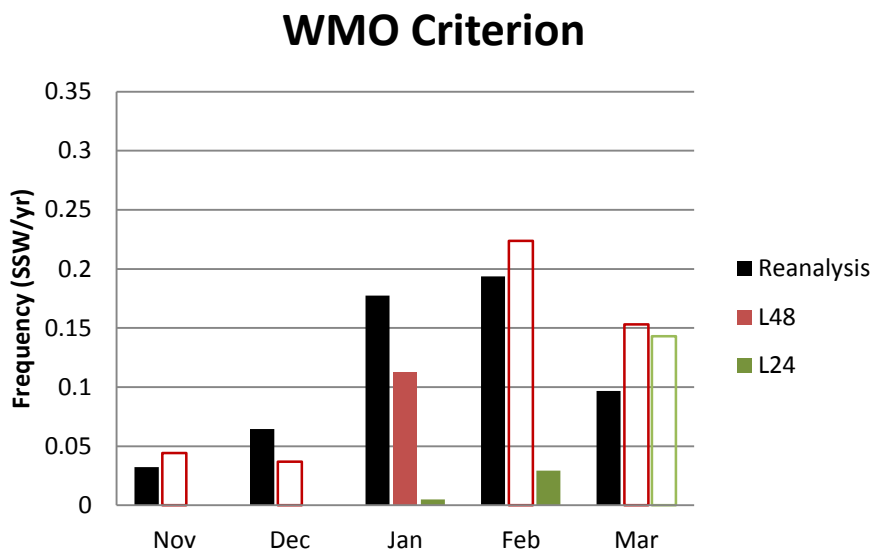


Figure 12. SSW frequency using the WMO criterion. See Figure 11 caption.

at SSW responses amid different SSW criteria, an analysis of SSWs is performed using the new SSW criteria we put forth.

As was seen Figure 12 with the WMO criterion, the L24 model did not reach the 0 m/s SSW threshold in early winter and has significantly less SSWs through the middle of winter compared to the reanalysis and L48 model data. Since the Magnitude criterion adjusts for the daily climatological difference in the mean strength of the vortex between the reanalysis and each model, this new SSW threshold allows SSWs to be counted more easily in the L24 model. As seen in Figure 13, the difference between the WMO and Magnitude criteria is most noticeable particularly in early and mid-winter in the L24 model where there is an increase in SSW frequency. In early winter for the L24, where no SSWs were detected using the WMO method, there are now detectable SSW events. However though SSWs see an increase in frequency, there is still a lower SSW frequency

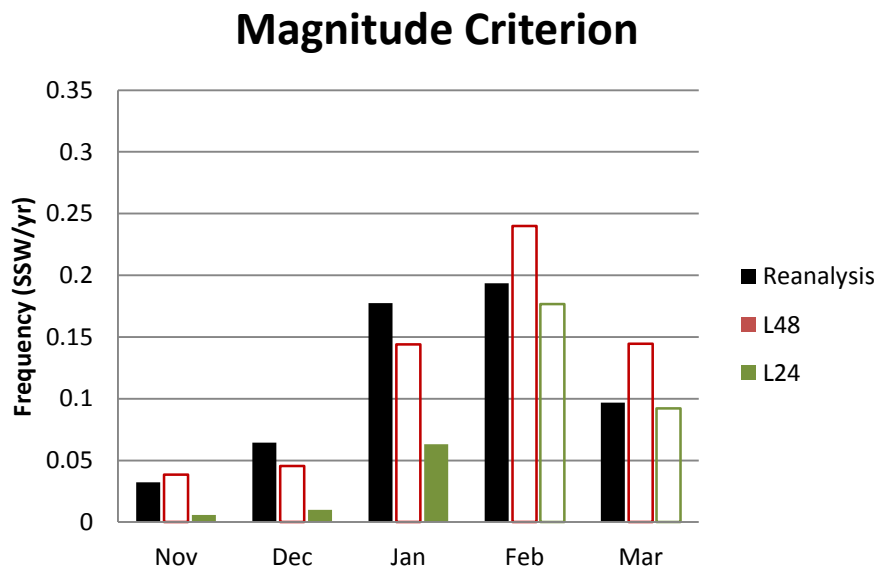


Figure 13. SSW frequency using the Magnitude criterion. See Figure 11 caption.

between L24 and other datasets. This leads us to believe that an underrepresentation of WMO SSWs is not solely a function of a stronger polar vortex but also its variability. In mid-winter, while SSW frequency relative to the reanalysis and L48 model is still lower, an increase is seen in the number of SSWs compared with the WMO criterion. Since an adjustment is made for the stronger vortex in the L24 model, results show that the Magnitude criterion is somewhat effective at making the frequency of SSWs less contingent on a changing mean strength of the polar vortex.

Like the Magnitude criterion, the Kinetic criterion takes the daily climatological difference between the reanalysis and model datasets. However, in this criterion the zonal wind is squared to make zonal-mean zonal wind proportional to kinetic energy. The daily difference between the two kinetic energy climatologies is used as the new threshold. From an energetic perspective it is clear that when the polar vortex is significantly stronger than the polar vortex found in the reanalysis, the SSW threshold is easier to reach. This is evident in Figure 14 where the L24 control run in early and mid-winter has a much higher SSW frequency compared to the reanalysis data. This difference is also seen in February. However the exception to this is March. No SSWs are detected in the L24 data and almost no SSWs are counted for the L48 data. This could possibly be attributed to the way March SSWs are confirmed as discussed in section 2.4. Although the threshold might be easy to break, the vortex must rebound and be above that threshold for 10 consecutive days in order to be counted as an SSW. The L48 model has a significant increase in December and January SSW frequency. These significant increases, especially in January, are likely due to the L48 model having a stronger vortex than the reanalysis data as seen in Figure 9. Ultimately due to the strong SSW biases

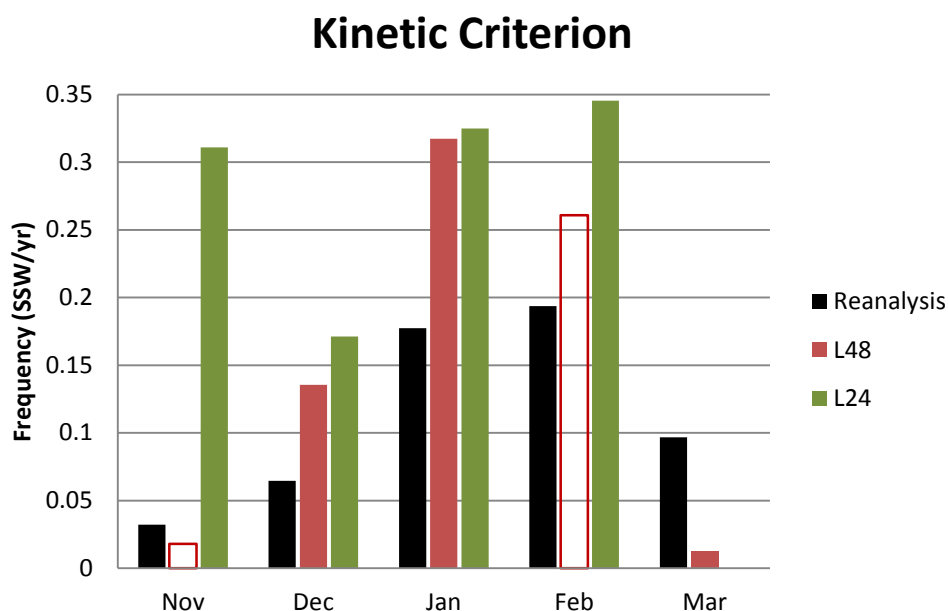


Figure 14. SSW frequency using the Kinetic criterion. See Figure 11 caption.

when the polar vortex winds are strong, we claim that this criterion is unreliable in the analysis of SSWs.

Unlike the other criteria, the Drop criterion (Figure 15) is not tied to the daily climatology of the polar vortex but counts an SSW as a 25 m/s or greater decrease in zonal-mean zonal winds within a week's timeframe. Overall, the reanalysis data has a seasonal SSW frequency peak in January while both models have an SSW frequency peak in February. This is consistent with the variability that is found between the reanalysis and models found in Figure 10 where reanalysis variability peaks earlier in winter than the models. The most noticeable differences between the datasets are the relatively low SSW frequency through November and December in the L24 and L48 models compared to reanalysis. This can also be reflected in Figure 10 as variability is lower than reanalysis until January. The L48 model has a much higher SSW frequency in

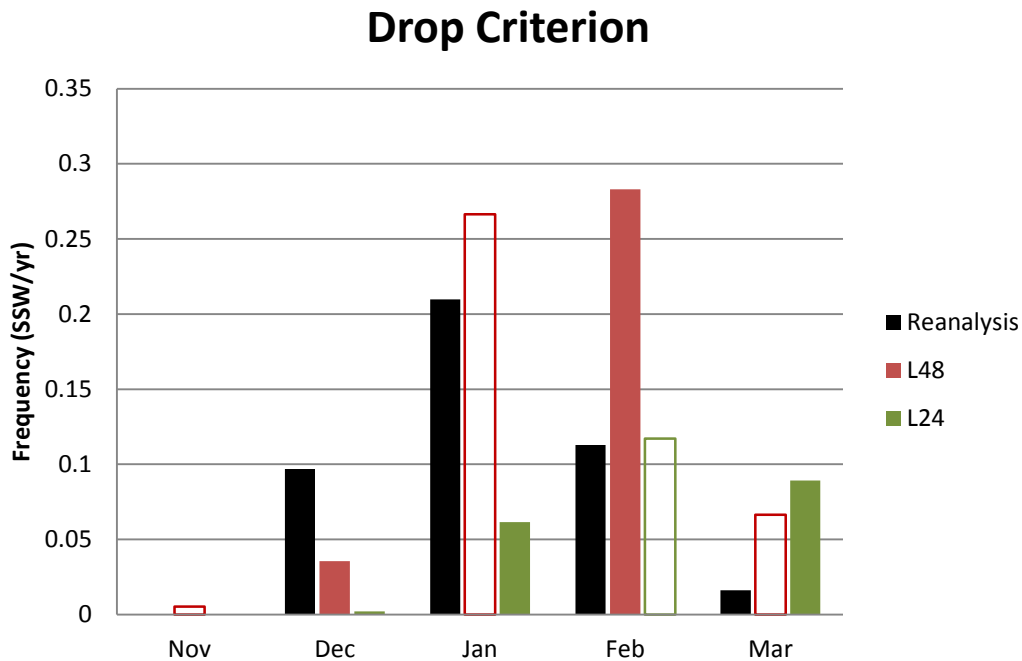


Figure 15. SSW frequency using the Drop criterion. See Figure 11 caption.

February compared with both the reanalysis and the L24 model. This can be partially attributed to differences in variability throughout February as the L48 model has a higher amount of variability during that timeframe than the L24 model and reanalysis. All in all, winter SSW frequency is highest in the L48 data while lowest in the L24 data. Seasonal frequency peaks in the reanalysis data occur in January while both the L24 and L48 models have SSWs peak in February.

The Kinetic Drop criterion (Figure 16) looks for a threshold of two times the squared value of zonal-wind drop that is investigated in the Drop criterion. Like the Drop criterion, the SSWs over all datasets in November are mostly absent due to a lower amount of variability in early winter. Unlike the Drop criterion though, all three datasets have a peak SSW frequency in January. This is like attributed to two factors. While the seasonal frequency of the Drop criterion is more closely related the seasonal variability of

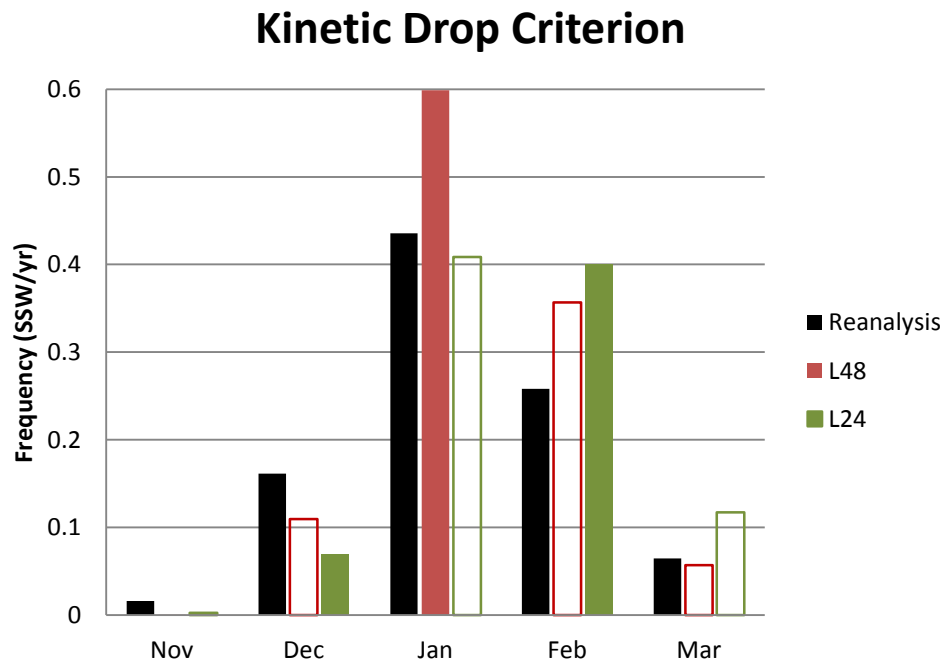


Figure 16. SSW frequency using the Kinetic Drop criterion. See Figure 11 caption.

each polar vortex, the Kinetic Drop criterion is contingent on both variability and strength of the vortex. This is because any increase (decrease) in u-wind velocity increases (decreases) the kinetic energy non-linearly since it is the squared value of the u-wind. With this being the case, where monthly frequencies are greater than those found in the reanalysis data it is likely due to that month having a stronger polar vortex along with variability. Additionally, the peak in SSWs for each dataset has been shifted to January and due to the two factors mentioned that allow for a lower or higher amount of SSWs. Also, all datasets have unrealistically higher SSW frequencies that are not necessarily indicative of a polar vortex breakdown. This leads us to conclude that the Kinetic Drop criterion is an unreliable criterion for identifying SSWs.

The NAM criterion identifies an SSW event when the NAM index reaches a threshold of -3. From Figure 11, despite a difference in the annual frequency between the

L24 model and reanalysis, no individual month has a statistically different frequency than reanalysis in Figure 17. However while there is no statistically significant individual month, the cumulative effect of most months having lower SSW frequencies than reanalysis likely makes the annual SSW frequency statistically significant. As is seen in both kinetic criteria the reanalysis and L48 have their seasonal peak in SSW frequency in January. The NAM criterion also matches well with all other criteria (except the WMO criterion) in the L24 model having a season SSW frequency peak in February.

3.4. Model Forcing Scenarios

The new SSW criteria we presented in the previous section will now be used to investigate potential SSW responses amidst different climate forcing scenarios for the L48 model. All results from the forcing experiments will be compared to the control

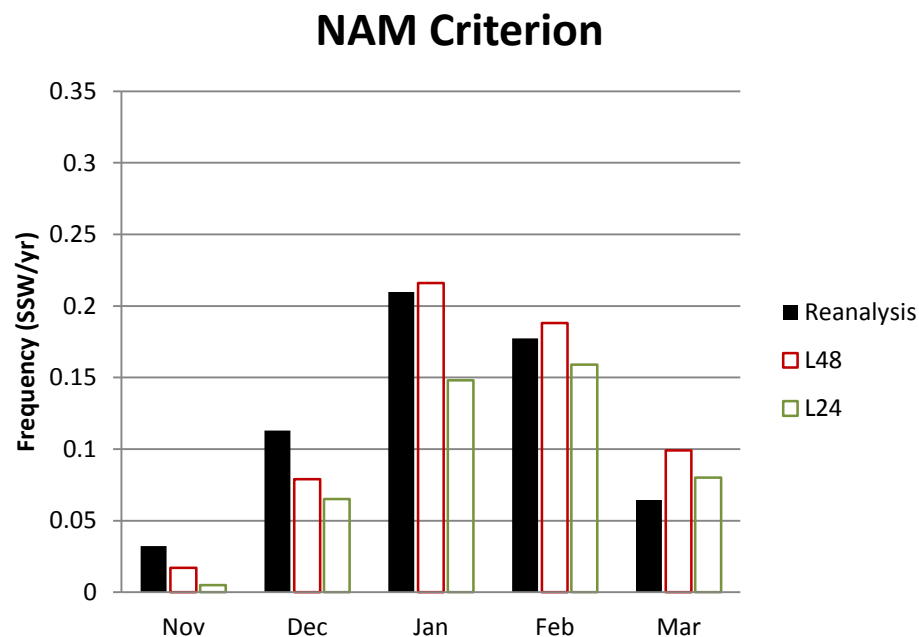


Figure 17. SSW frequency using the NAM criterion. See Figure 11 caption.

(preindustrial) run in terms of percentage change. Before this is addressed, a look at each scenario's daily zonal-mean zonal wind climatology and variability is done to understand how the polar vortex during winter is changing in both strength and variability.

3.4.1 Zonal-Mean Zonal Wind Climatology

The mean strength of the polar vortex for each forcing scenario is investigated in Figure 18 and 19. In October as the polar vortex continues to develop, there is an increase (decrease) in the strength of the vortex as the CO₂ concentrations in each forcing scenario are increased (decreased). This is also prevalent in the first half of November before all scenarios have a similar vortex in the second half of November. For December through February winds decrease as CO₂ concentrations increase. Late February and March, as

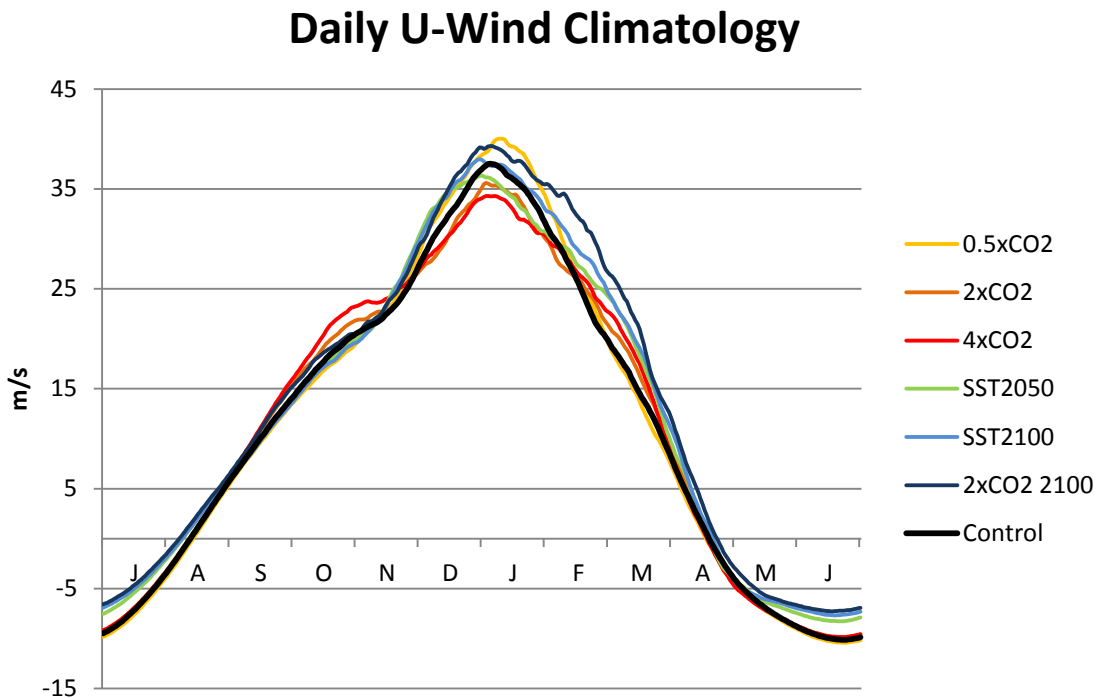


Figure 18. Daily mean zonal-mean zonal wind climatology (m/s) at 60°N and 10 hPa

Daily U-Wind Climatology Anomalies

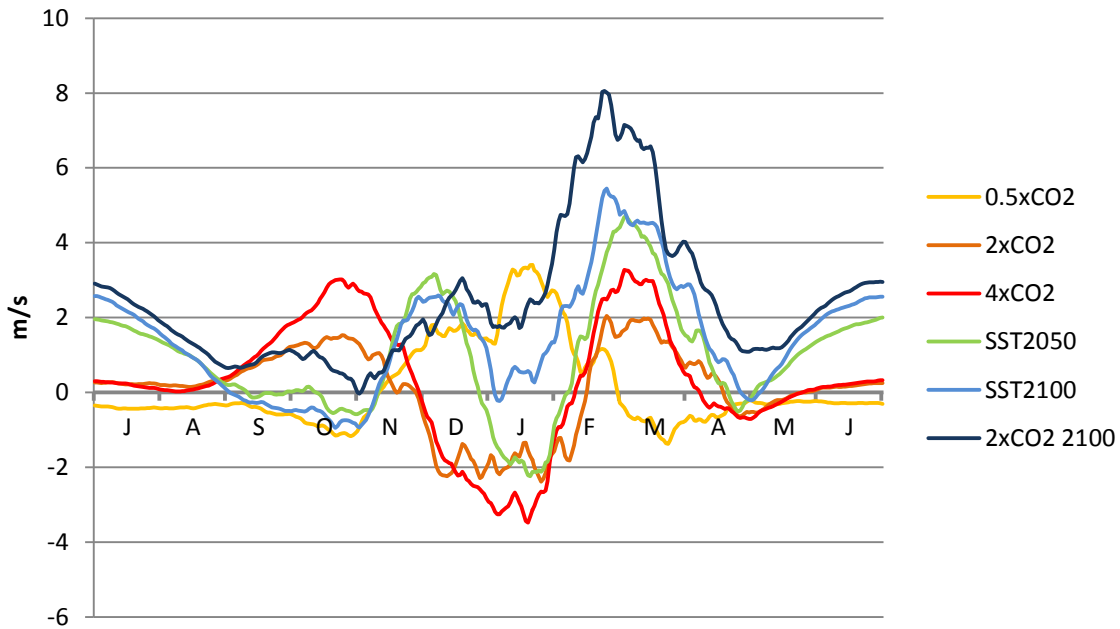


Figure 19. Daily mean zonal-mean zonal wind climatology (m/s) at 60°N and 10 hPa.

the polar vortex starts to transition from its winter to summer state, a similar behavior is found when the polar vortex decreases as when it strengthened in October and early November: when concentrations are increased in each scenario the mean strength of the polar vortex also increases. All in all, as CO₂ concentrations increase, the winter bench seasons see a mean strengthening of the polar vortex while DJF see a weakening of the vortex.

For the SST scenarios, there is no noticeable difference from the control run over fall months as the polar vortex strengthens. For November and December all future SST forcing simulations show a stronger vortex than the control run while in January only the 2xCO₂_2100 run has a stronger vortex than the control run. This trend continues into spring as the 2xCO₂_2100 run vortex is much stronger than all other runs. Increasing

SSTs alone in the SST2050 and SST2100 runs show no considerable change from the control run until February. By late winter all SST runs have a stronger vortex than the control run. After investigating the mean strength of the polar vortex in each forcing scenario, a proposed question discussed earlier can be addressed by looking at the variability of each forcing scenario: is a change in the mean strength of the vortex due to the vortex strength actually changing or because of a change in SSW frequencies over that same period.

3.4.2 Mean Seasonal Variability

Figure 20 and 21 displays the daily average standard deviation of the zonal-mean zonal wind for all forcing scenarios. For the CO₂ scenarios, as CO₂ concentrations increase, variability also increases particularly from October to mid-January. In late

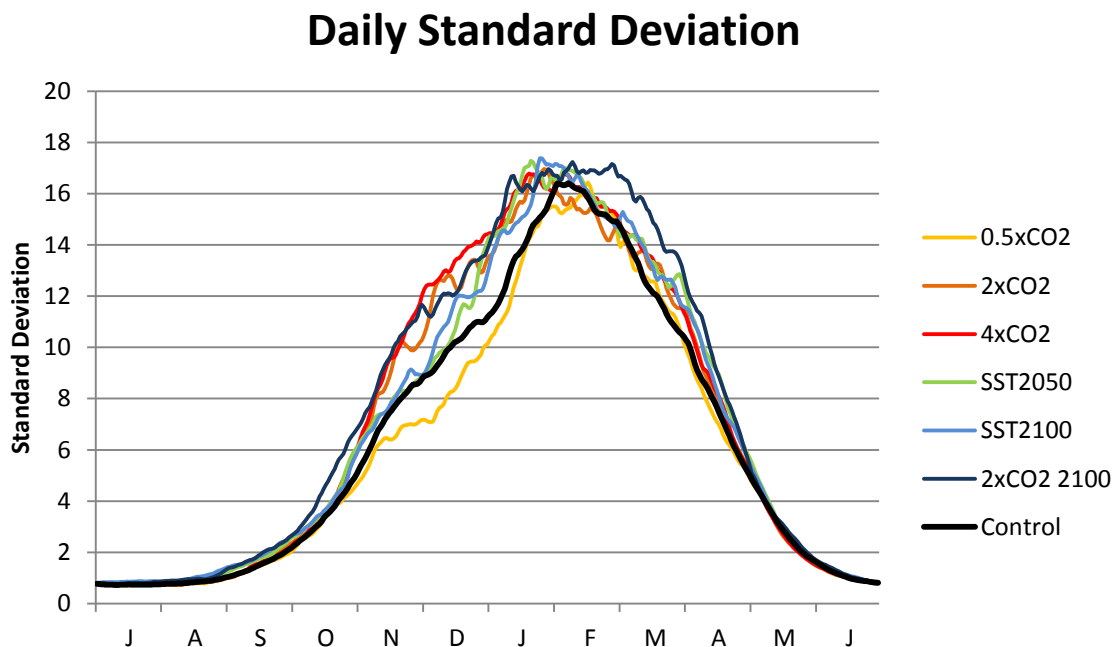


Figure 20. Daily mean standard deviation for the zonal-mean zonal wind at 60°N and 10 hPa for July thru June.

Daily Standard Deviation Anomalies

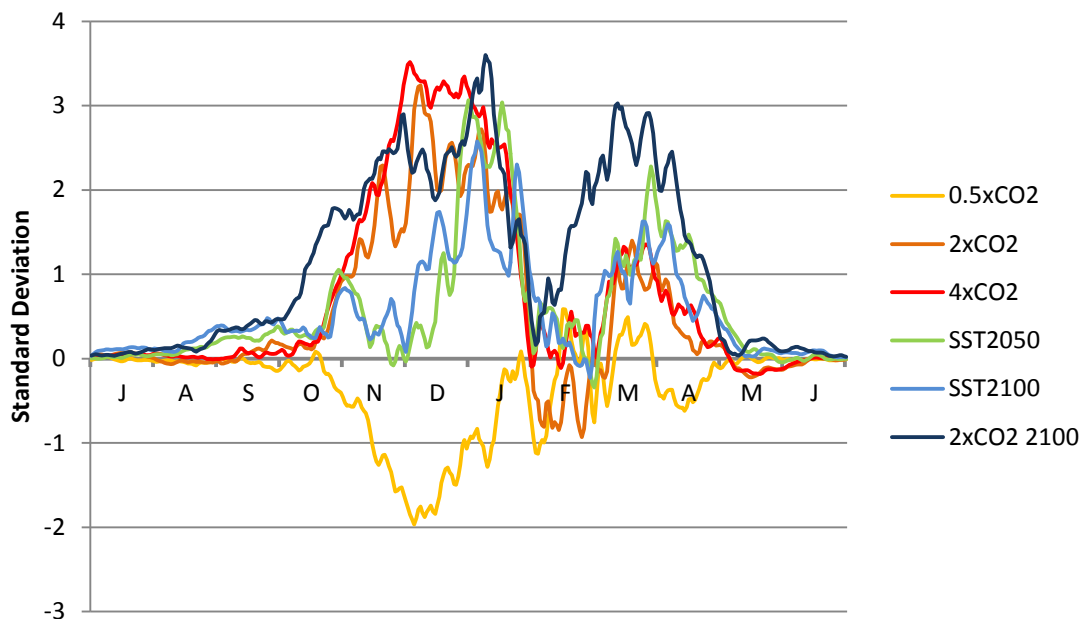


Figure 21. Daily mean standard deviation anomalies based off control run for the zonal-mean zonal wind at 60°N and 10 hPa for July thru June.

winter and spring there is slightly higher variability in the 2xCO₂ and 4xCO₂ scenarios, but overall the different variability between all CO₂ scenarios is much smaller when compared to fall and early winter.

For the SST scenarios, as SSTs increase, the variability does as well from early fall into January. In early February the SST2050 and SST2100 scenarios have similar variability and remain similar for the remainder of winter and spring. The SST scenario that has a significantly higher daily variability in late winter into spring when compared to the control run and other SST scenarios is the 2xCO₂_2100 scenario. Throughout the timeframe this model run has a higher amount of variability.

The trend of increased variability from November through January as CO₂ concentrations and SSTs increase can also be seen in Figure 10 between the reanalysis and L48 model control run data. From the L48 control run (SST and CO₂ conditions from

the year 1860) to the reanalysis data (years 1948-2010) there is an increase in variability in early through mid-winter. Though the sampling size is limited in the reanalysis data, this variability increase in fall and early winter is consistent with both the L48 SST and CO₂ scenarios.

In analyzing both the daily mean zonal wind and daily variability, the question proposed in section 2.3 is addressed: Does weaker daily zonal wind climatology cause more WMO SSWs due to the mean winds needing to drop less in order to reach the 0 m/s threshold or does the daily climatology decrease due to more SSWs? We claim that if the zonal wind changes along with the variability, no conclusions can be made in terms of what causes what. However we think that if there is a decrease (increase) in the zonal-mean zonal wind climatology while an increase (decrease) is seen in variability, the decrease (increase) in zonal wind climatology can be caused by an increase (decrease) in the frequency of polar vortex breakdowns. This will be reflected in the monthly SSW frequency responses later in this section.

3.5 Annual SSW Frequency Comparison

After investigating the daily mean strength of the polar vortex and its daily average variability, we now look at the annual and then monthly SSW response to climate forcing scenarios for each SSW criterion.

3.5.1 SSW Annual Frequency Summaries

Overall for the CO₂ scenarios, no matter which way an SSW is defined there is an increase in SSW frequency when CO₂ concentrations are increased (Figure 22). The 0.5xCO₂ run shows a significant decrease in SSWs in the WMO criterion which would be consistent with its stronger polar vortex and lower variability but only in the NAM

L48 Annual SSW Frequency Change

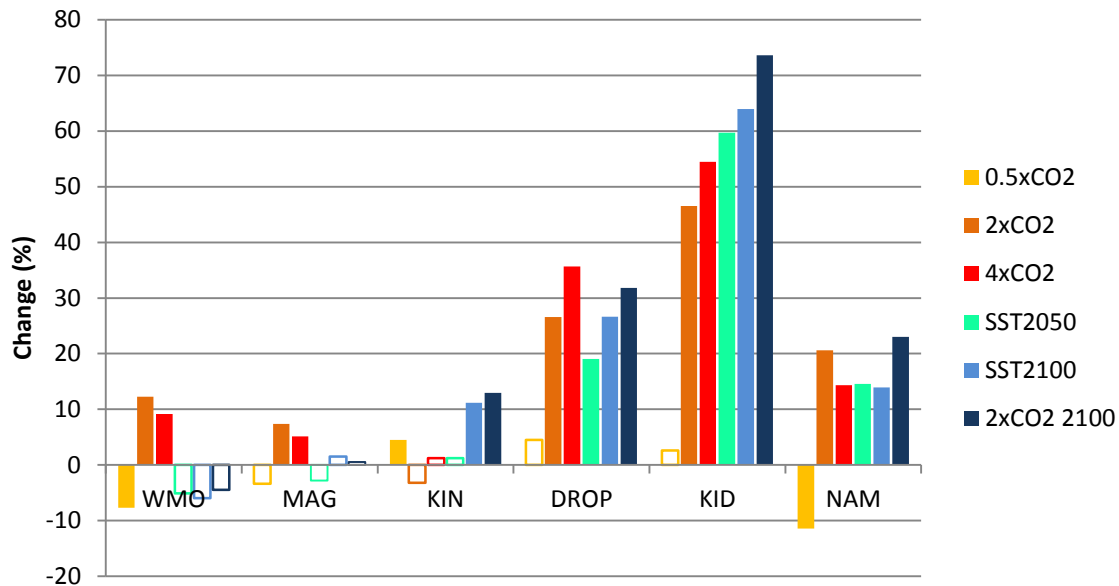


Figure 22. Comparison of annual SSW frequency (SSW/yr) percent change of L48 model forcing scenarios from the control run. Filled boxes signify a 95% statistically significant difference from L48 model control run.

criteria are similar results seen. Interestingly, the Kinetic criterion shows an increase in SSWs with the Kinetic Drop criterion also showing a similar increase, albeit statistically insignificant, for the 0.5xCO₂ run. As discussed in section 3.3 this can be attributed to the stronger polar vortex the 0.5xCO₂ run has (Figure 18) which makes the SSW threshold in both kinetic energy criterion easier to break.

With the exception of the WMO and Magnitude criteria, when SSTs are increased there is also an increase in SSW frequency. Since both the SST2050 and SST2100 have a stronger vortex but also greater standard deviation for the first half of winter and also in March, it is reasonable that the SSW frequency in the WMO criterion remains unchanged. Similar results are seen in the Magnitude criterion as well. However, this too seems reasonable since, for example, the mean strength of the polar vortex

increases ~ 5 m/s while the standard deviation only increases by ~ 1.5 . Though the Magnitude criterion adjusts for the mean strength of the polar vortex, the variability does not proportionally increase leaving the SSW frequency unchanged from the control run.

When CO_2 is added in the $2\times\text{CO}_2_{2100}$ scenario in every criterion it has the highest increase in SSW frequency out of the SST scenarios with the exception of the WMO criterion. Since the SST2100 scenario not only has the strongest but also the most variable vortex, the lack of SSW response is likely attributed to the same reasons stated above for the SST2050 and SST2100 scenarios.

3.5.2 Monthly SSW Frequency Response

We now investigate and compare the monthly SSW response for all six criteria starting with the WMO criterion (Figure 23). For the CO_2 forcing scenarios there is a significant increase in SSW frequency as CO_2 concentrations are increased from November through January. These results are consistent with the clear variability increase in the first half of winter when CO_2 concentrations are increased in Figure 20 and Figure 21. In February there is an opposite behavior potentially signifying a shift in the seasonal peak of SSWs; when CO_2 concentrations increase there is a gradual decrease in the amount of SSWs in the month. However while this February pattern is clear, results do not become statistically significant until the $4\times\text{CO}_2$ run. In March there is a clear increase in frequency when concentrations are decreased as found in the $0.5\times\text{CO}_2$ run; however, there is no significant response when they are increased. Overall for the CO_2 forcing scenarios, SSWs appear to increase in frequency when CO_2 concentrations increase in early to mid-winter while a reduction in SSWs occurs in late winter and early spring.

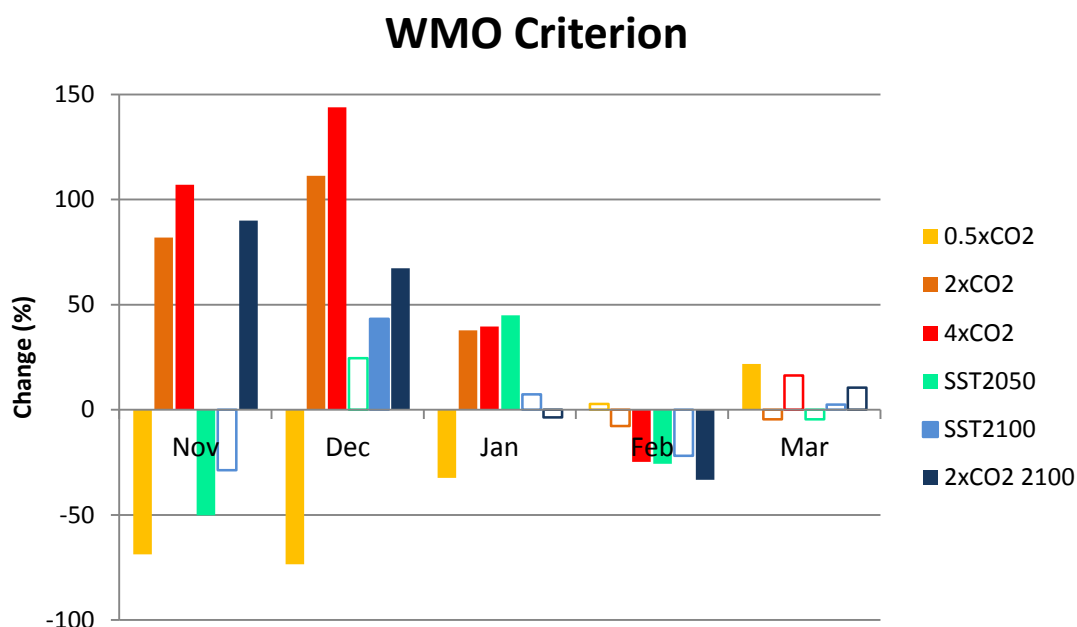


Figure 23. Comparison of WMO criterion monthly SSW frequency (SSW/yr) percent change of L48 model forcing scenarios from the control run. Filled boxes signify a 95% statistically significant difference from model control run.

For SST forcing scenarios when SSTs are increased there is a reduction in SSWs in November. For December, SSWs remaining statistically similar to the control run. The only statistically significant increase in frequency in both November and December is seen when CO₂ concentrations are doubled in the 2xCO₂_2100 scenario. All SST forcing scenarios see a significant decrease in SSW frequency in February while March frequencies remain unchanged from those found in the control run.

The Magnitude criterion (Figure 24) shows a similar pattern in the CO₂ scenarios as was found in the WMO criterion. Despite adjusting the daily threshold based on a stronger or weaker polar vortex climatology when CO₂ levels increase there is still an increase in early and mid-winter SSWs. The decrease in February SSWs where CO₂ increases found in the WMO criterion is still significant in the 4xCO₂ run. There is also,

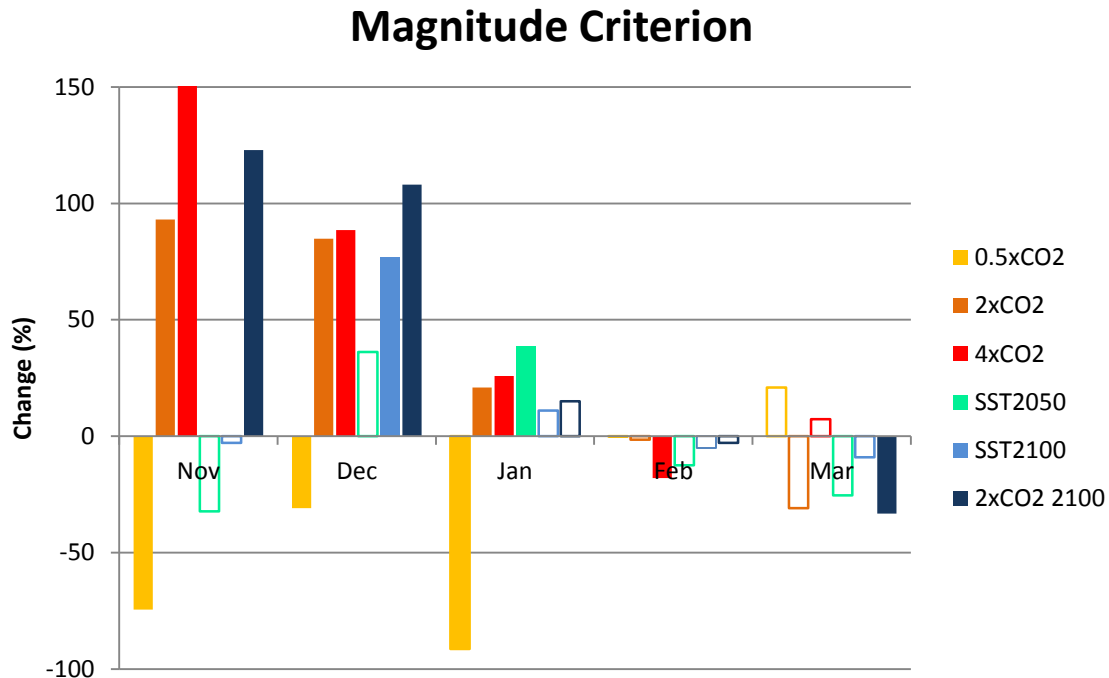


Figure 24. Comparison of Magnitude criterion monthly SSW frequency (SSW/yr) percent change of L48 model forcing scenarios from the control run. Filled boxes signify a 95% statistically significant difference from reanalysis run.

like in the WMO criterion, an increase in frequency when CO_2 concentrations are decreased in the 0.5xCO_2 run in March. In spite of the Magnitude criterion adjusting for any change in the mean state for the polar vortex the same pattern of increasing and decreasing SSWs in early and late winter as the WMO criterion is found. With that being said, though the pattern is similar, the magnitude of the SSW frequency changes from the control run is changed by the Magnitude criterion.

For the SST scenarios there exists some slight changes from the SSW frequency results found in the WMO criterion. are now statically insignificant from the control run. In December when SSTs are increased in the SST2100 run, there is now a statistically significant increase in SSWs. For both months the 2xCO_2_{2100} has a greater frequency increase than that found in the WMO criterion. This result, can be expected because

although the polar vortex is stronger, allowing for an SSW threshold to be greater than 0 m/s, the variability also increased proportionally allowing for more SSWs to occur. This scenario not only can be seen in the $2xCO_2_{2100}$ results but in others frequency responses as well. A more noticeable difference between the two criteria is the SSW frequencies in February. Where the WMO criterion had all three SST scenarios with lower SSW frequencies than the control run, the Magnitude criterion SSWs see no change from the control run. Another significant difference is found in March in the $2xCO_2_{2100}$ run. The WMO criterion has SSWs in March insignificantly decreasing from the control run but in the Magnitude criterion there is a statistically significant decrease. This is an interesting result as the variability also increases with the increased strength of the vortex in March. However, like the lower March SSW frequencies in for the Kinetic criterion in the previous section, this decrease is likely the byproduct of the added March criterion that separates SSWs from SFWs.

When looking at the polar vortex through an energetic perspective with the Kinetic criterion in Figure 25 it is apparent there are dramatic increases in SSW activity in early winter. For the sake of graphic appearance, the bounds of the chart remain the same as the previous two SSW criterion charts despite frequencies in November increasing upwards of 400 percent as few SSWs are found in the control run. With the exception of the $0.5xCO_2$ run that shows a decrease in SSWs, all scenarios show an increase in frequency in November. For CO_2 scenarios in December and January, there is a clear decrease in SSW frequency as CO_2 concentrations increase. This pattern of decreasing SSWs can best be explained by a weaker vortex found over these months in the increasing CO_2 scenarios. As discussed earlier, if the vortex is significantly stronger

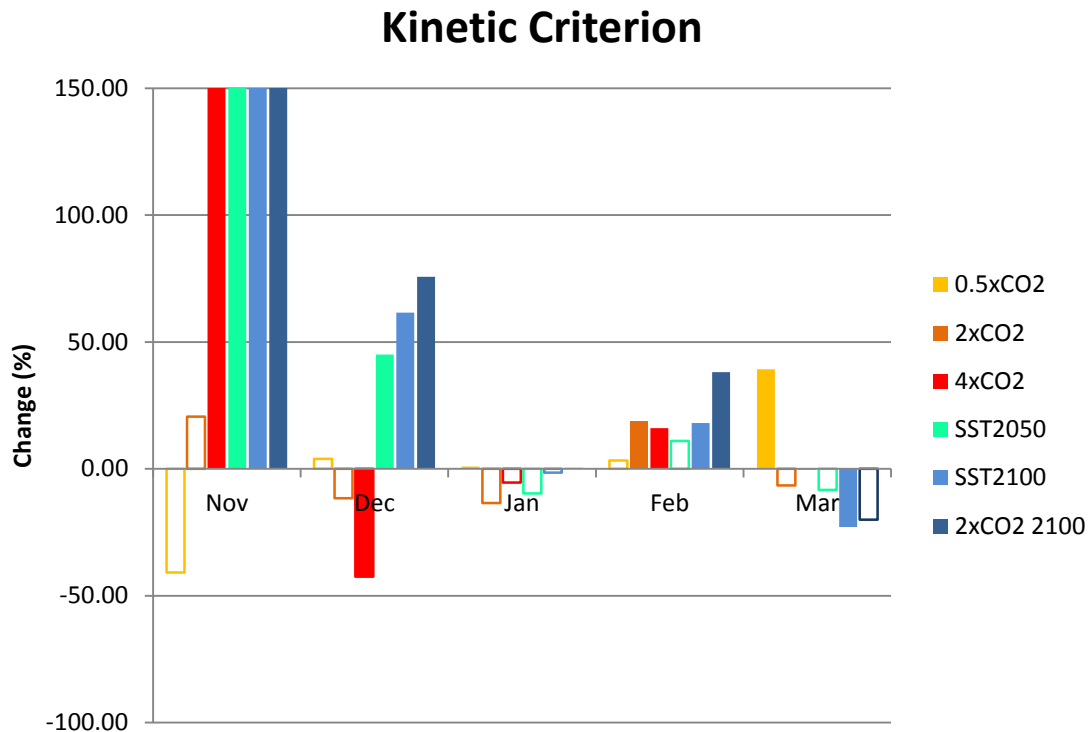


Figure 25. Comparison of Kinetic criterion monthly SSW frequency (SSW/yr) percent change of L48 model forcing scenarios from the control run. Filled boxes signify a 95% statistically significant difference from reanalysis run.

than the control run vortex, it is likely that more SSWs will be counted. The same decreasing pattern is also found in March as well while February shows an increase in SSW frequency when CO₂ concentrations are also increased. Overall for the CO₂ scenarios, there is a clear increase in SSWs in November and February when CO₂ concentrations are increased while a decrease is seen in December, January, and March.

For the SST scenarios, there is an increase in SSW frequency from the control run in almost all scenarios from November, December, and February. The only month where a significant decrease in SSW frequency is seen is in March likely the byproduct of the added March SSW criterion. The largest SSW frequency change in the SST scenarios,

which is also seen in the CO₂ scenarios, occurs in early winter while changes in SSW frequency are less extreme towards late winter.

Like the Kinetic criterion, the Drop criterion (Figure 26) also has a large increase in SSW frequency in early winter. For the CO₂ scenarios, the 0.5xCO₂ run has no SSWs occurring in November while the 2xCO₂ and 4xCO₂ runs have large frequency increases. This can be attributed the lower amount of SSWs detected in the control run since a 25 m/s drop in November is unlikely (which can be a potential downside to the criterion). For December and January, a similar pattern exists as is also found in November. When CO₂ concentrations increase, there is a significant increase in SSWs. While a decreasing frequency pattern could be identified in February, the CO₂ scenarios are statistically similar to the control run. All CO₂ forcing scenarios show an increase in frequency in March however the 4xCO₂ run has a significantly higher frequency change than the other

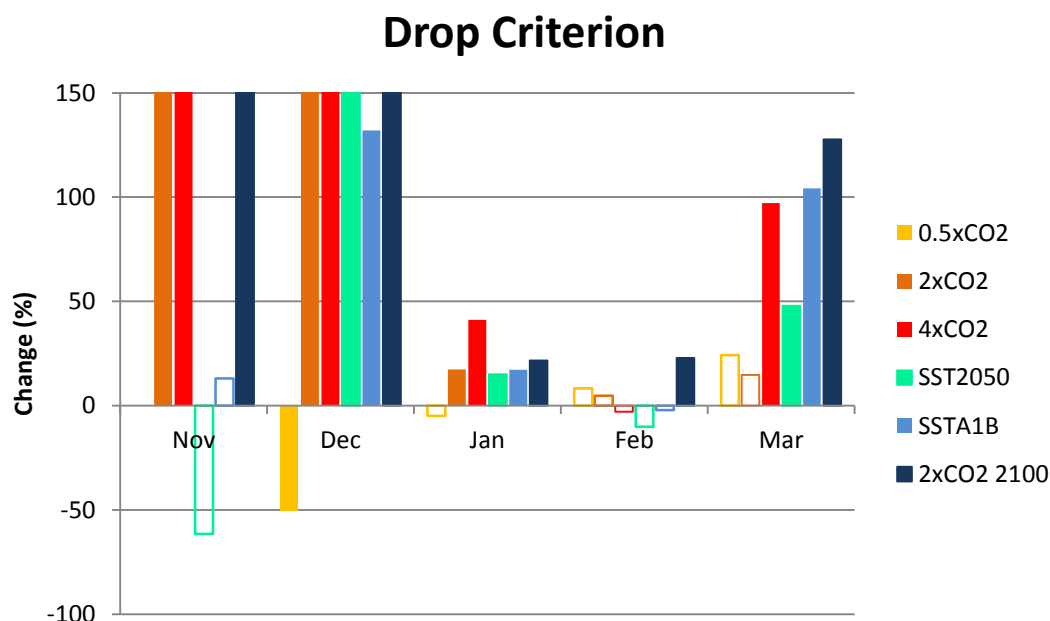


Figure 26. Comparison of Drop criterion monthly SSW frequency (SSW/yr) percent change of L48 model forcing scenarios from the control run. Filled boxes signify a 95% statistically significant difference from reanalysis run.

CO₂ scenarios.

For SST scenarios in November, when SSTs are increased there is no statistically significant difference between the control run and SST forcing scenarios. Only when CO₂ is added in the 2xCO₂_2100 run, is there a significant increase in frequency. For December and January all three SST scenarios show a SSW frequency increase. February shows no change from the control run for the SST2050 and SST2100 run while the 2xCO₂_2100 run than the control run. For both the CO₂ and the SST forcing scenarios the largest changes in SSW frequency can be found in both early to mid-winter and March. Particularly in early winter, this result is consistent with all SSW criteria implemented thus far and is also consistent with Figure 20 that shows variability increasing as well.

In the control run there are no SSWs detected using the Kinetic Drop criterion in November (Figure 27). Therefore, any SSWs counted will result in large frequency increases as are found in both the 4xCO₂ and the 2xCO₂_2100 runs. For December, CO₂ scenarios show an increase in frequency when CO₂ concentrations are increased. For January and February most CO₂ scenarios show no change in frequency from the control run. March has a large increase in SSW frequency only in the 4xCO₂ run. As discussed earlier about the Drop Kinetic criterion, a combination of a stronger vortex, plus increased variability over March will cause a significant increase in the amount of SSWs counted. Like the Drop criterion, the largest increases for the CO₂ scenarios are seen in early winter and March.

For the SST scenarios, all runs show a significant SSW frequency increase when SSTs are increased in December and March. Like most of the CO₂ scenarios there is no SSW frequency change in the SST2050 and the SST2100 run when compared to the

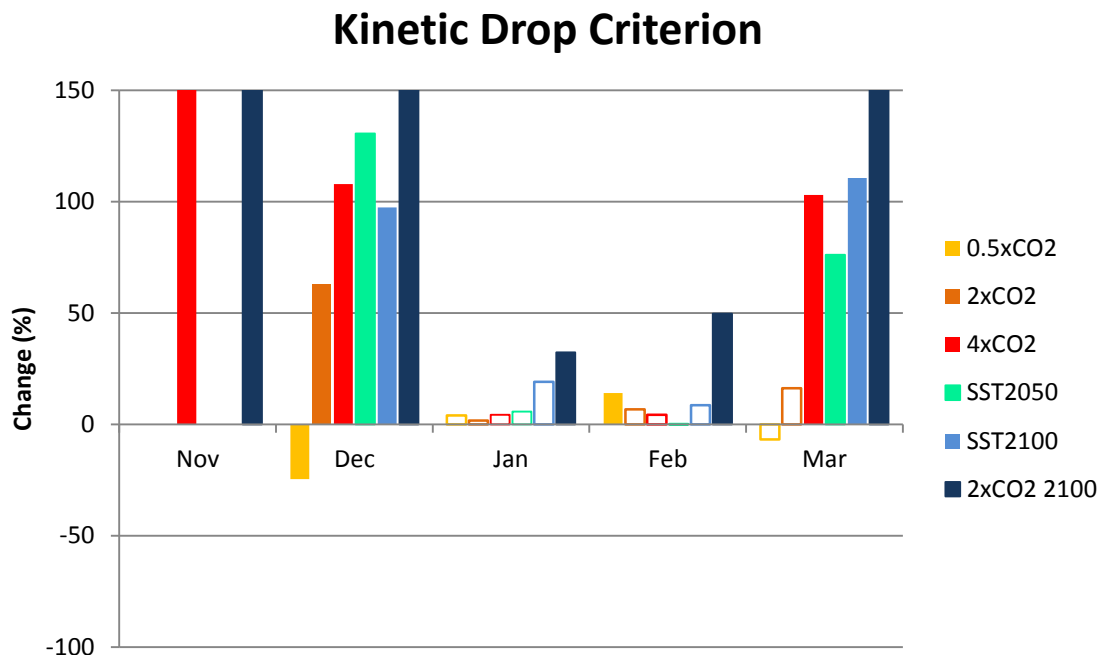


Figure 27. Comparison of Kinetic Drop criterion monthly SSW frequency (SSW/yr) percent change of L48 model forcing scenarios from the control run. Filled boxes signify a 95% statistically significant difference from reanalysis run.

control run in January and February. The 2xCO₂_2100 run is the only run that shows a significant increase in frequency in mid-winter.

As seen in the previous criteria and as well in the NAM criterion (Figure 28), when CO₂ is increased there is an increase in SSW frequency in November and December. With the exception of a significant decrease in SSW frequency for the 4xCO₂ in February for Figure 28, all CO₂ runs have a similar monthly frequency to the control run from January through March. The cause of the decrease in SSW frequency in the 4xCO₂ scenario in February is unknown as during this timeframe the variability is similar to the control run while the strength of the vortex is slightly stronger. The overall pattern of SSW frequency increase is in line with the other criteria, particularly the frequency

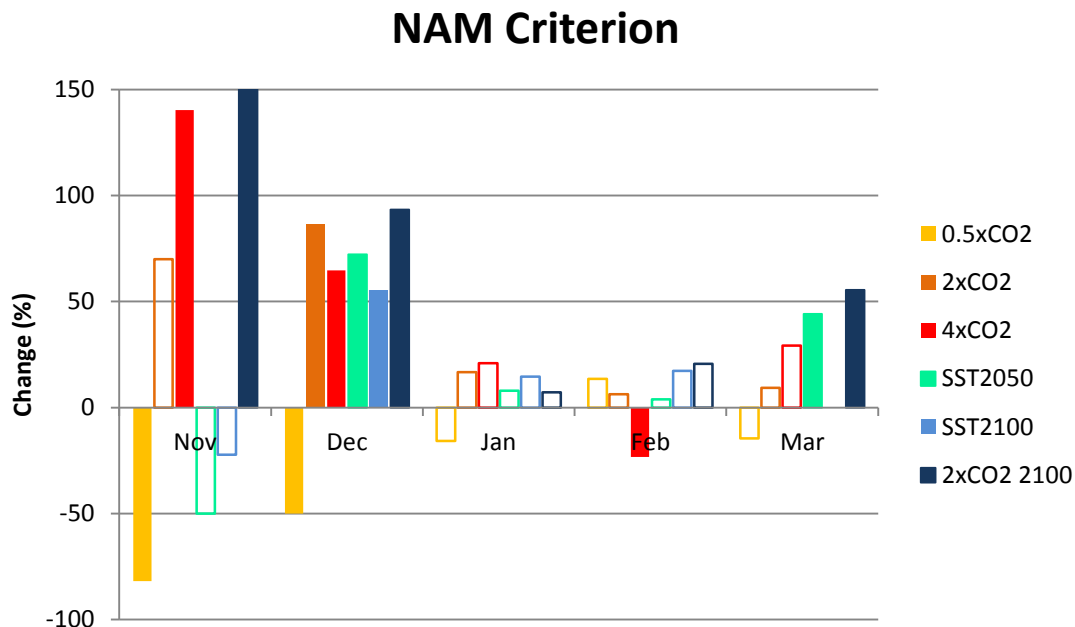


Figure 28. Comparison of NAM criterion monthly SSW frequency (SSW/yr) percent change of L48 model forcing scenarios from the control run. Filled boxes signify a 95% statistically significant difference from reanalysis run.

increase in early winter.

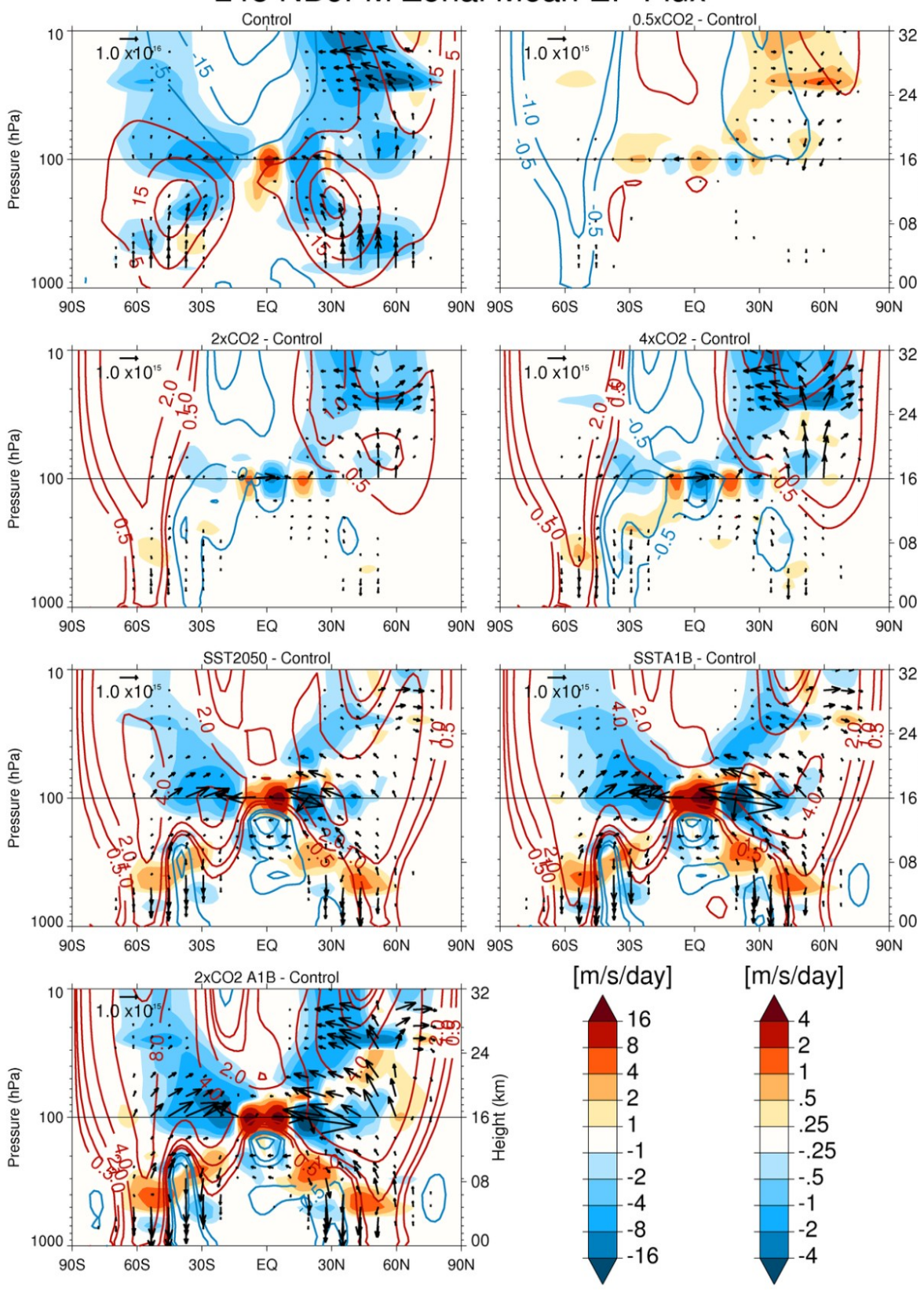
For the SST scenarios, there is a significant increase in SSW frequency for all SST runs in December. For January and February there is no significant change in frequency while March shows a significant increase in the SST2050 and 2xCO₂_2100 runs. There is also no change in March SSW frequency between the control run and SST2100 run.

3.6 SSW Dynamical Response to Forcing Scenarios

Since the upward propagation of tropospheric wave energy into the polar stratosphere is the primary cause of SSWs, an analysis of EP-fluxes and the amount of convergence of wave energy into the polar stratosphere is investigated. Figure 29 shows

Figure 29. Average difference in EP-Flux, divergence, and zonal-wind for each forcing scenario. Y-axis is log-pressure height with latitude on x-axis. Eliassen-Palm flux arrows with reference arrows for the control are 1×10^{16} (kg/s^2) for the control run and 1×10^{15} (kg/s^2) for all other panels. Nonfilled colored contours are zonal-mean zonal wind values (m/s). Filled colored contours are the convergence (blue) and divergence (red) values (m/s/day). Winter mean values in the control run are then subtracted from each forcing scenarios. Area above 100 hPa horizontal line is multiplied by a factor of 10 for stratospheric analysis.

L48 NDJFM Zonal Mean EP Flux



the direction of tropospheric wave energy in the meridional cross-section represented by EP-flux vectors and their convergence/divergence from November through March. The control run panel shows that the majority of upward propagating wave energy into the stratosphere is diverted equator ward.

When subtracting the winter mean vectors, EP-flux convergence/divergence, and zonal wind values of the control run from those of the $0.5\times\text{CO}_2$ run there is a reduction in the amount of convergence in the polar stratosphere. This can also be seen in terms of the vectors that are pointed both downward and equatorward indicating not only that there is a reduced amount of tropospheric wave energy propagating upward into the stratosphere but also the amount that is moving into the poleward into the vortex is decreasing. When CO_2 concentrations are increased the opposite results occur. There is an increase in the amount of EP-flux convergence into the polar stratosphere as well as an increase in the amount of upward and poleward moving wave energy.

When SSTs are increased the stratospheric response is not as robust as is seen in the CO_2 scenarios. With that being said however, there is still a slight increase in the amount of upward moving wave energy and a slightly larger increase in the amount of poleward moving energy. With some regions of the polar stratosphere seeing divergence and others experiencing convergence, it is visually unclear if there is an overall net change in the EP-flux convergence/divergence in the polar stratosphere region. When CO_2 is doubled in the $2\times\text{CO}_2_{2100}$ run convergence in the polar stratosphere as well the amount of upward and poleward wave energy that propagates into the vortex are increasing.

As discussed in section 2.2.2, to quantify the change between scenarios seen in Figure 29, the percentage change of upward wave energy into the stratosphere and the change of the convergence of wave energy into the polar vortex between forcing scenarios are calculated and displayed in Figure 30 and Figure 31.

Whether observing Figure 30 through a monthly or winter season perspective, there is an increase in the amount of upward propagating wave energy in almost every forcing scenario with the exception of the 0.5xCO₂ run. This upward wave energy generally increases when either CO₂ concentrations or SSTs are increased. As is seen in the difference of EP-flux vectors between the control run and forcing scenarios in Figure 29 that show stratosphere vectors pointing poleward, not only is there an increase in

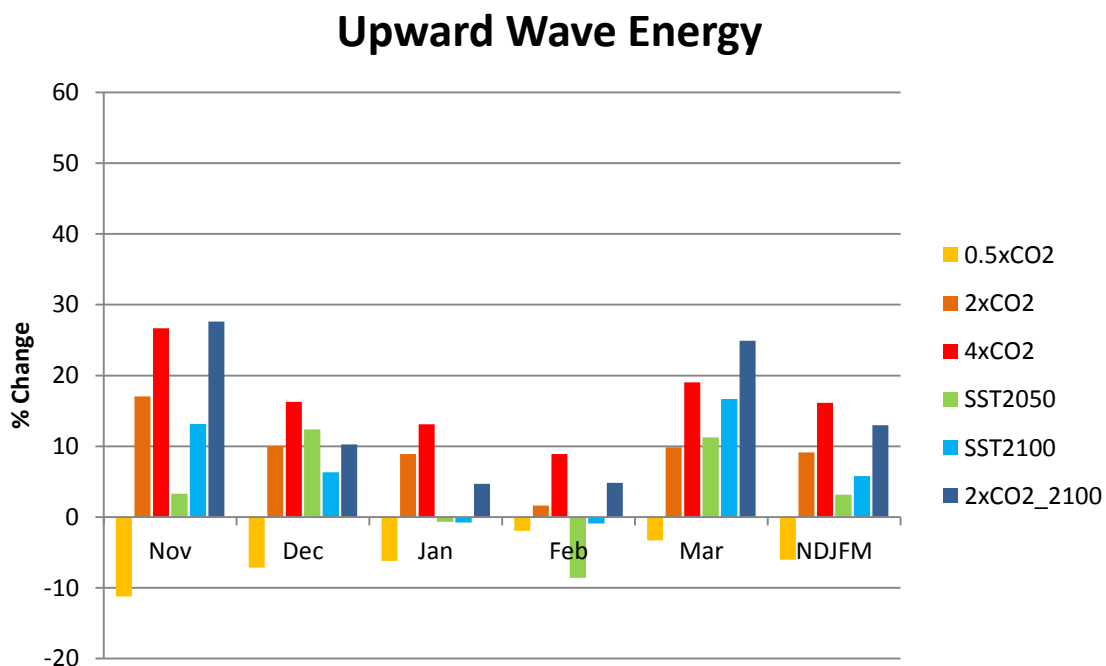


Figure 30. Seasonal and annual percentage change of upward wave energy from control run.

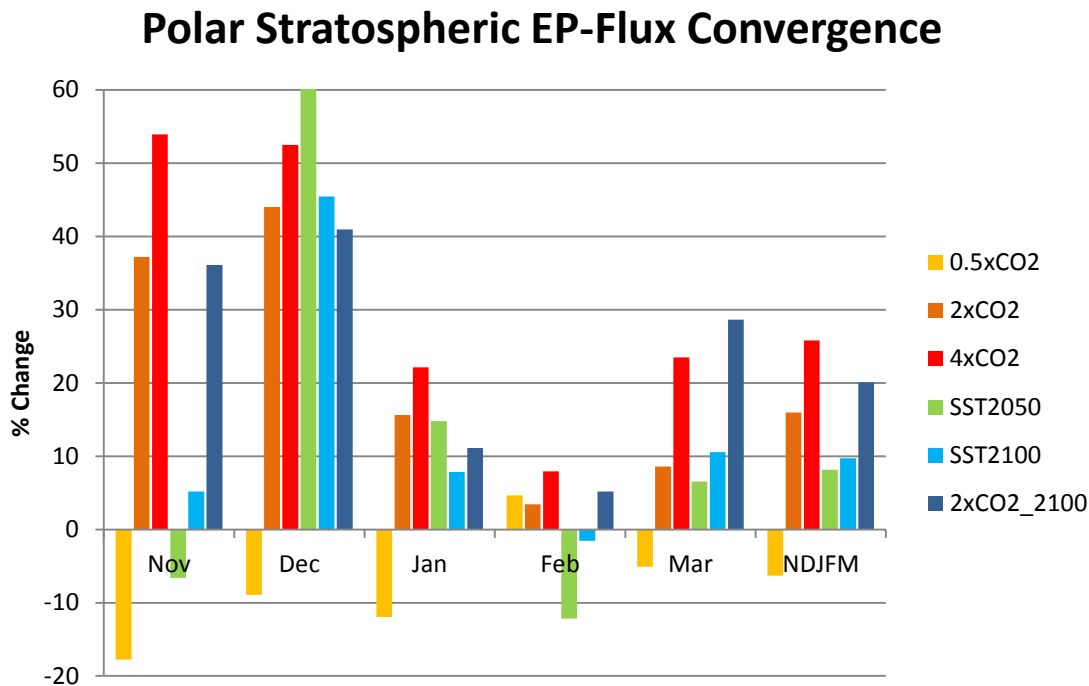


Figure 31. Seasonal and annual percentage change of polar stratospheric EP-flux convergence from control run.

upward wave energy but also in the poleward transport of wave energy. This can likely explain the greater increase in the amount of polar stratosphere EP-flux convergence than is seen in to upward wave energy. There is not only an increase of upward wave energy but also an increase (decrease) in the amount of wave energy that is moving poleward (equatorward).

From a monthly perspective, the largest increase in polar stratospheric convergence is seen in early winter when either CO₂ concentrations or SSTs are increased. This is consistent with an increase in early winter SSWs that is seen in every SSW criteria investigated in this study. The smallest amount of change in polar stratosphere EP-flux convergence is seen in February. This too is reflected in most SSW

criteria with February being the month of lowest frequency change. March also has an increase in convergence however this increase is not reflected in all SSW criteria due to the added March SFW criterion. Only the Drop, Kinetic Drop, and NAM criteria have an increase in SSW frequency that matches the magnitude increase seen in polar stratosphere EP-flux convergence in Figure 31.

From a winter season perspective, there is a somewhat linear increase in convergence seen in the 2 and 4xCO₂ runs. This is correctly replicated in almost all the SSW criterions however only the WMO and Magnitude criterion replicate the decrease in convergence seen in the 0.5xCO₂ run. The convergence increase seen in the SST forcing scenarios is also seen in all criterions except the WMO and Magnitude criteria due to the stronger polar vortex explained earlier. Though the convergence of tropospheric wave energy into the stratosphere is the primary reason for SSWs, the increase in SSWs is not similar in magnitude to the increase in polar stratospheric convergence. This, as explained earlier, is more of a function of how the SSW criteria have certain biases that make SSWs more or less likely to occur.

3.7 Analysis and Comparison of C20R and NCEP-NCAR Reanalysis Data

The polar vortex in the NCEP-NCAR reanalysis (NNR) and C20R are compared to investigate how well the C20R can be used for stratospheric analysis. The strength of the polar vortex between the two datasets is compared in Figure 32 using data between 1948 and 2010. The C20R polar vortex is not only significantly stronger than the NNR vortex but also has a different seasonality. The NNR vortex has a peak in strength in late December and early January whereas the C20R has its peak strength in late January into early February. The variability seen in Figure 33 also has a similar shift. Peak variability

Daily U-Wind Climatology

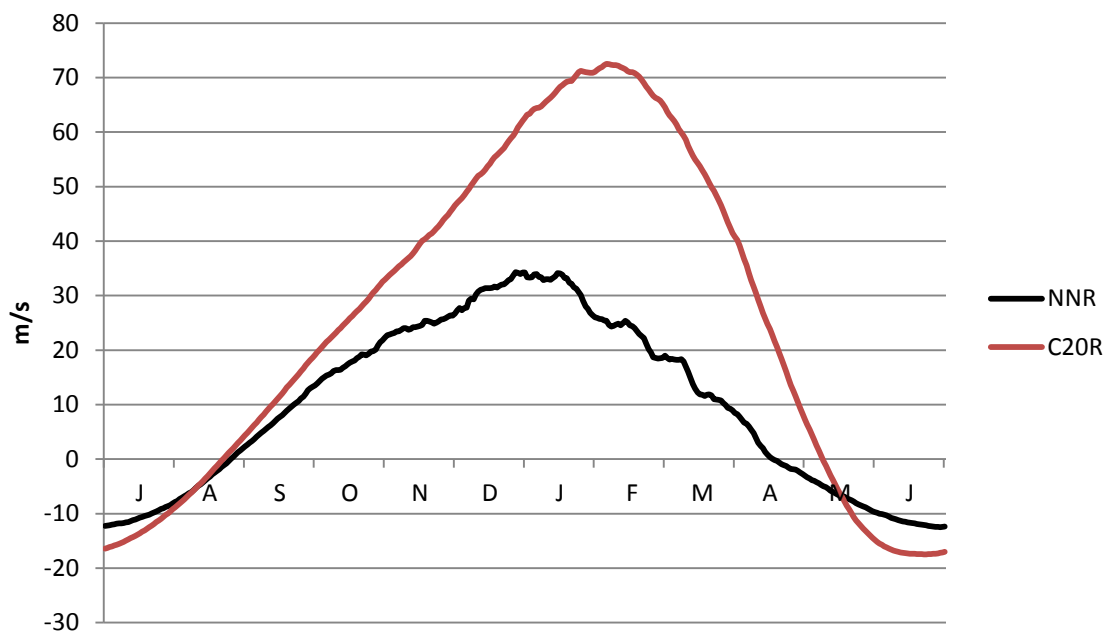


Figure 32. Zonal mean u-wind daily climatology at 10 hPa and 60N.

Daily Standard Deviation

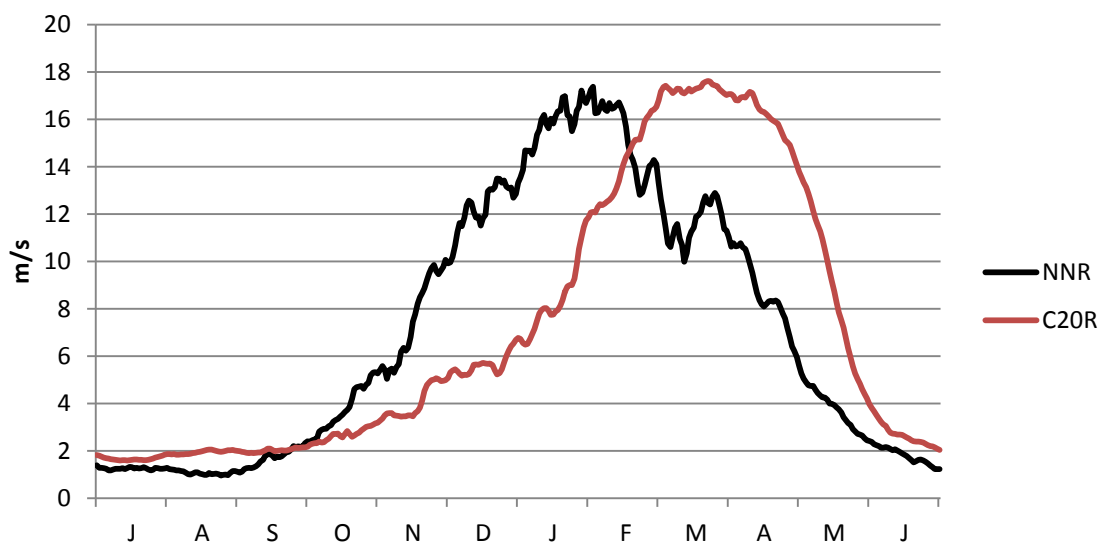


Figure 33. Zonal mean u-wind daily standard deviation climatology at 10 hPa and 60N.

in the C20R vortex occurs approximately two months after the peak seen in NNR. Also, the variability between the two datasets is similar in magnitude. Considering the polar vortex found in the C20R is more than twice as strong as the NNR vortex it reveals how the C20R vortex is less prone to vortex breakdown than the NNR vortex.

A correlation is also performed for the same timeframe for the zonal-mean zonal wind at 60°N and 10 hPa and the NAM index at 10 hPa in order to see how well the C20R replicates the stratospheric variability found in the NNR. As seen in Table 2 it is clear that the C20R data do not accurately replicate the NNR polar stratosphere as all correlations coefficients are under 0.3. Even years when NNR satellite-based observation data is isolated (1979-present) there is a very low correlation between the two datasets. Seeing that this correlation is so low, no SSW analysis is performed.

Table 2: Correlation coefficients between NNR and C20R.

| | 1948-2010 | 1979-2010 |
|---------------|------------------|------------------|
| U-Wind | 0.285 | 0.255 |
| NAM | 0.208 | 0.213 |

4. SUMMARY AND DISCUSSION

In summary, we first sought to develop and test alternative methods for identifying stratospheric sudden warming events (SSWs). This was motivated by the apparent shortcoming of the World Meteorological Organization (WMO) criterion as highlighted by McLandress and Shepherd (2009); if the strength of the polar vortex is stronger than observation, the frequency of SSWs will be less by definition. To address Objective 1, we tested our alternative SSW criteria using data from reanalysis, a high-top and a low-top model control run. Through this analysis we found that most of our alternative SSW criteria led to reliable results except the criteria based on kinetic energy; they are overly sensitive to biases in the strength of the polar vortex. This shortcoming was most evident using data from the low-top model under an unrealistically strong polar vortex.

To answer Objective 2, we next applied our alternative criteria to long climate change time slice simulations using the high-top model. We found that increases in CO₂ concentrations or warming SSTs general led to an increase in annual mean SSW frequency. In contrast, using the WMO criterion the frequency of SSWs declined when warming SSTs because the stronger zonal winds made the WMO threshold more difficult to break. We also analyzed changes in SSW frequency during individual months which revealed that increases in SSWs were particularly large in early to mid-winter (November thru January). By investigating Objective 3, we further found that the increase in SSW frequency was accompanied by a consistent increase in the amount of upward

propagating wave energy and a convergence of that energy into the polar stratosphere. This consistent behavior was found both on annual mean data and in monthly data.

Lastly for Objective 4, we analyzed a long reanalysis dataset spanning the entire 20th century to examine if the dataset could provide useful information about the past history of SSWs. Through comparing this dataset to the more conventional reanalysis dataset we found that the 20th century dataset poorly replicated the real time stratosphere and was not good for SSW analysis.

The main result from this study is that most of our alternate SSW definitions indicate an increase in SSW frequency as climate is forced by increasing CO₂ concentrations or warming SSTs. This increase is largest in early to mid-winter, which is consistent with the findings of Bell et al. (2010) and Mitchell et al. (2012). Our results are very robust with respect to the details of how SSWs are defined. Both an increase in early and mid-winter zonal wind standard deviation and wave energy converging into the polar stratosphere give us reason to believe that the increased SSW frequency is not solely a byproduct of the criteria put forth in this study. We also, however, observe an increase in wave energy convergence in March, which was not always apparent in our monthly SSW frequency results. We conclude that the “Drop” and “NAM” criterion were best at replicating this increased variability and wave convergence due to the way SSWs are differentiated from stratospheric final warming events in March.

We also conclude that out of the new criteria we put forth there are some criteria that are less reliable than others. We assert that the “Magnitude” and kinetic energy criteria are not very reliable SSW criteria. As mentioned earlier, kinetic energy criteria overproduce SSWs especially when there are strong zonal-mean zonal winds. The kinetic

energy criteria SSW results are not reflected in the daily mean variability nor in the amount of converging wave energy into the polar stratosphere which give us reason to believe any SSW response is more a byproduct of the criteria biases. Similar to the shortcoming of the WMO criterion, kinetic energy criteria are also even more contingent on the zonal wind climatology. The “Magnitude” criterion we think is also not reliable. This is because the zonal wind climatologies that are derived from forcing scenarios to adjust the SSW threshold are also modulated by changes in the frequency of SSWs. Due to the above reasons, we think that the “Magnitude” and kinetic energy criteria should not be used in the analysis of SSWs in future climate scenarios.

We also think that there are several SSW criteria that are more reliable: the “Drop” and “NAM” criteria. From an annual perspective they replicate the increased wave energy convergence seen by increasing CO₂ concentration or warming SSTs. From a monthly perspective both criteria have SSW responses that replicate the changes in the daily mean standard deviation and also the monthly changes seen in wave energy convergence. We think that the “Drop” and “NAM” criteria have the least amount of criteria biases and also sufficiently replicate the changes in both the annual and seasonal increase in polar vortex variability and wave convergence.

Practically, we assert that our results lead us to expect that in future climate conditions there will be an increase in variability in the polar vortex particularly in winter bench months of early to mid-winter and March. Since the polar vortex can modulate the surface AO and frequency of cold air outbreaks, we expect that the increase in stratospheric variability will also lead to increased variability in mid-latitude and polar surface temperatures over these same timeframes. As previous authors have concluded,

this means an increased potential for cold air outbreaks for mid-latitude regions such as North America, Europe, and northern Asia.

There are several potential shortcomings to this study. Although the results of increased variability and SSW frequency from an annual and seasonal perspective are consistent with previous studies, we only perform an analysis of these SSW criteria on one model, the GFDL AM2.1. There would be increased confidence in these results if more models would not only verify the variability seen in our model but also show a similar SSW response using the criteria put forth in this study. Furthermore, the prescribed SSTs used in our forcing scenarios are taken from the A1B scenario. This scenario, however, is just one of many of the possible future climate scenarios that can occur. This gives us reason to believe that future SST scenarios in this study are a source of uncertainty and a potential shortcoming. Another potential shortcoming of this study would be the implementation of our alternative SSW criteria in a transient model or for operational use. Several of our criteria can only be derived when the future climatological state of the stratosphere is known. Only in a GCM run in equilibrium is this viable.

We put forth several possible research extensions for this study as well. As mentioned above, performing this same analysis with the same SSW criteria using a different model would be desirable. Also, since it has been shown by various authors that stratospheric geopotential height anomalies tend to propagate from the stratosphere into the troposphere, an analysis of which criteria are most effective at capturing these downward propagating events when the polar vortex breaks down could be beneficial for operational forecasters. In addition, it would be of interest to investigate whether the

frequency of downward propagating SSWs is changing in response to climate forcings in similar ways as what was found in this study for SSWs.

REFERENCES

- Anderson, J.L., and Coauthors, 2004: The New GFDL Global Atmosphere and Land Model AM2 LM2: Evaluation with Prescribed SST Simulations. *J. Climate*, **17**(24):4641–4673
- Andersen, S. B. and B. M., Knudsen, 2006: The Influence of Polar Vortex Ozone Depletion on NH Mid-Latitude Ozone Trends in Spring, *Atmos. Chem. Phys.*, **6**, 2837-2845, doi:10.5194/acp-6-2837-2006.
- Andrews, D. G., J. R. Holton, and C. B. Leovy, 1987: *Middle Atmospheric Dynamics*. Academic Press, 260 pp.
- Baldwin, M., and T. Dunkerton, 1999: Propagation of the Arctic Oscillation from the Stratosphere to the Troposphere, *J. Geophys. Res.*, 104(D24), 30937-30946.
- Belchansky, G. I., D. C. Douglas, N. G. Platonov, 2004: Duration of the Arctic Sea Ice Melt Season: Regional and Interannual Variability, 1979–2001. *J. Climate*, **17**, 67–80.
- Bell, C., L. Gray, and J. Kettleborough, 2010: Changes in Northern Hemisphere Stratospheric Variability Under Increased CO₂ Concentrations. *Royal Meteorological Society* **136**, 1181-1190.
- Black, R.X., B.A. McDaniel, and W.A. Robinson, 2006: Stratosphere-Troposphere Coupling During Spring Onset. *J. Climate*, **19**, 4891-4901.
- Butchart, N., and Coauthors, 2006: Simulations of Anthropogenic Change in the Strength of the Brewer-Dobson Circulation. *Climate Dyn.*, **27**, 727–741, doi:10.1007/s00382-006-0162-4.
- Charlton, A. J., and Coauthors, 2007: A New Look at Stratospheric Sudden Warmings. Part II: Evaluation of Numerical Model Simulations. *J. Climate*, **20**, 470–488.
- Compo, G. P., J. S. Whitaker, and P. D., Sardeshmukh, 2006: Feasibility of a 100 Year Reanalysis Using Only Surface Pressure Data, *Bull. Am. Meteorol. Soc.*, **87**, 175–190, doi:10.1175/BAMS-87-2-175.
- Delworth, T.L., and Coauthors, 2006: GFDL's CM2 Global Coupled Climate Models. Part I: Formulation and Simulation Characteristics. *J. Climate*, **19**(5), 643–674

Kalnay, E., and Coauthors, 1996: The NCEP/NCAR 40-Year Reanalysis Project. *Bull. Amer. Meteor. Soc.*, **77**, 437–471.

Kolstad, E.W., T. Breiteig, A.A. Scaife, 2010: The Association Between Stratospheric Weak Polar Vortex Events and Cold Air Outbreaks in the Northern Hemisphere. *Q. J. R. Meteorol. Soc.* **136**: 886–893. DOI:10.1002/qj.620

McLandress, C., T.G. Shepherd, 2009a: Impact of Climate Change on Stratospheric Sudden Warmings as Simulated by the Canadian Middle Atmosphere Model. *J. Climate* **22**: 5449–5463.

Mitchell D.M., and Coauthors, 2012: The Nature of Arctic Polar Vortices in Chemistry–Climate Models. *Q. J. R. Meteorol. Soc.* DOI:10.1002/qj.1909

Staten, P. W., J. Rutz, T. Reichler, and J. Lu, 2011: Breaking Down the Tropospheric Circulation Response by Forcing. *Clim. Dyn.*, DOI-10.1007/s00382-011-1267-y.

Taguchi, M., 2003: Tropospheric Response to Stratospheric Sudden Warmings in a Simple Global Circulation Model. *J. Climate*, **16**, 3039–3049.

Thompson, D. W. J. and J.M. Wallace, 2000: Annular Modes in the Extratropical Circulation. Part I: Month-to-Month Variability*. *J. Climate*, **13**, 1000–1016.

Thompson, D.W. J., M.P., Baldwin, J.M., Wallace, 2002: Stratospheric Connection to Northern Hemisphere Wintertime Weather: Implications for Prediction. *J. Climate*, **15**, 1421–1428.

Wang, X., R.K. Jeffrey, 2005: Arctic Surface, Cloud, and Radiation Properties Based on the AVHRR Polar Pathfinder Dataset. Part I: Spatial and Temporal Characteristics. *J. Climate*, **18**, 2558–2574.

Wilks, D., 2006: *Statistical Methods in the Atmospheric Sciences*. Academic Press, 141 pp.